Fermi National Accelerator Laboratory

FERMILAB-FN-577

A Study of Tunes Near Integer Values in Hadron Colliders

P. Zhang

Fermi National Accelerator Laboratory
P.O. Box 500, Batavia, Illinois 60510

December 1991

Operated by Universities Research Association Inc. under Contract No. DE-AC02-76CHO3000 with the United States Department of Energy

Disclaimer

A STUDY OF TUNES NEAR INTEGER VALUES IN HADRON COLLIDERS

ABSTRACT

The benefits and difficulties associated with operating a hadron collider with betatron tunes near integer values are investigated. The benefits are due to the larger area in betatron tune space which is free of lower order resonances. An experiment with the Tevatron P-$\bar{P}$ collider at Fermi National Accelerator Laboratory indicated that operating with tunes near 19.06 allowed a tune shift four times greater than the one allowed with the normal Tevatron working point near 19.42. In principle, this new working point should increase the maximum luminosity by a factor of sixteen. Difficulties with the new working point include reduced luminosity lifetime. In particular, the lower betatron frequencies associated with tunes near the integer have a greater overlap with the power supply noise spectrum which leads to transverse emittance growth. The effects of power supply noise were investigated with the Tevatron P-$\bar{P}$ collider. A feedback system was developed to reduce common-mode noise on the main power supply bus which reduced emittance growth rates. The mechanism for the common mode excitation of the beam growth was investigated using a superconducting magnet in the Magnet Test Facility at Fermilab.

ACKNOWLEDGEMENTS

I wish to express my thanks to my advisor, Professor Shoruko Ohnuma for his continual guidance, invaluable help and firm support in this work. More importantly, it is his exemplarily persistent pursuit and vigorous enthusiasm toward scientific objectives from which I draw much inspiration and encouragement.

It is a great pleasure to sincerely thank my other dissertation committee members: Professors M. Gorman, B. Pettitti, L. Pinsky and G. Reiter for their support.

I am grateful to the members in Accelerator Physics Committee of Fermi National Accelerator Laboratory for allowing me the opportunity to participate in their program, especially to Drs. A. Tollestrup, J. Peoples, G. Dugan, M. Harrison and R. Rubinstein for their support, approval of the project and the precious Tevatron beam time.

My special thanks go to Drs. A. Tollestrup, C. Ankenbrandt, D. Finley and K-Y. Ng for many enlightening conversations. I would also like to thank C. Ankenbrandt, D. Finley, G. Goderre, G. Jackson, D. Wolff, D. Siergiej and M. Kuchnir for their help in the experiments.

Over all, I wish to express my sincere thanks and deep appreciation to my advisor Dr. Rolland Johnson for directing my research work and for his unlimited help, encouragement and support throughout this work.

TABLE OF CONTENTS

LIST OF FIGURES

LIST OF SYMBOLS

B	magnetic field
B'	the gradient of magnetic field
$B\rho$	magnetic rigidity
C	the circumference of an accelerator
D	dispersion function
e	the charge of proton
f	the focal length of quadrupole magnet (thin lens approximation)
k	the error of focusing function
K	focusing function
l	the length of a magnet
P	proton
$\bar{P}$	antiproton
s	longitudinal variable
α	lattice parameter
β	lattice parameter
β_r	relativistic factor
γ	lattice parameter
γ_r	relativistic factor
$\Delta p/p$	momentum spread
ε_v	permittivity constant

ϵ	emittance
ϵ_N	$= \epsilon/(\gamma_r \beta_r)$, normalized emittance
μ_v	magnetic permeability
μ	one turn phase advance of betatron oscillation
ν	$\equiv \mu/(2\pi)$, tune of betatron oscillation
ξ	$\equiv d\nu/(\Delta p/p)$, chromaticity
ρ	the radius of curvature
σ	the rms beam size
ϕ	$\equiv \psi/\nu$, normalized phase advance
ψ	phase advance of betatron oscillation

CHAPTER I

INTRODUCTION

This dissertation is a study of a new working point in betatron tune space for hadron colliders. The study was motivated by the desire to improve the performance of hadron colliders for high energy physics experiments. One example of such a machine is the Proton-Antiproton (P -$\bar{P}$) Tevatron Collider at Fermi National Accelerator Laboratory (Fermilab).[1] All of the working point experiments described in this work have been performed with the superconducting Tevatron Collider.

1.1 Accelerator parameters relevant to high energy physics experiments

High energy physics experiments require a large center-of-mass (CM) energy and a high counting rate for the creation of new massive particles as well as for other rare events.[2] Modern hadron colliders provide higher CM energy than fixed target machines. If two relativistic particles of total energy E_1 and E_2 circulate in opposite direction in a storage ring, the amount of available energy for a particle creation in head-on collisions is given by

$$E_{CM} \approx \sqrt{4E_1E_2}. \qquad (1-1)$$

If $E_1 = E_2$, the center of mass of the collision is at rest in the laboratory. In such a machine virtually all the energy is available for the particle creation and the CM energy rises as E instead of as $\sqrt{E}$ in a fixed target machine.[3][4] At present, the highest available CM energy is 1.8 TeV in the Tevatron Collider: a 0.9 TeV proton beam collides head-on with a 0.9 TeV antiproton beam travelling in the opposite direction in the same ring.

The counting rate $\mathcal{R}$ of an event in a collider is the product of its cross section $\sigma_{p\bar{p}}$ and the luminosity $\mathcal{L}$, which is a collider parameter.

$$\mathcal{R} = \sigma_{p\bar{p}} \cdot \mathcal{L}. \qquad (1-2)$$

For a given cross section, the total number of events N available for analysis is proportional to the integrated counting rate and depends on the time variation of the luminosity described by luminosity lifetime,

$$N = \int \mathcal{R}dt = \sigma_{p\bar{p}} \cdot \int \mathcal{L}(t)dt. \qquad (1-3)$$

Therefore, peak luminosity and luminosity lifetime along with CM energy are important collider parameters for high energy physics experiments. To achieve a higher total number of events, one may increase the center of mass energy since the $P\bar{P}$ cross section increases with energy.[5] It is however difficult to increase the energy of a collider once the collider is built since the achievable maximum energy is determined by the machine radius and the peak magnetic field. We can, however, improve the machine performance by increasing the peak luminosity or the luminosity lifetime, or both at the same time.

1.2 Motivation of the work

The luminosity of a collider is proportional to the number of particles N_p and $N_{\bar{p}}$ of each bunch, the beam revolution frequency f_{rev}, the number of bunches N_B and inversely proportional to the square of the beam size σ (round beam assumed),

$$\mathcal{L} \propto \frac{f_{rev} N_p N_{\bar{p}} N_B}{\sigma^2}. \qquad (1-4)$$

At each crossing point, strong electromagnetic forces generated by one beam perturb transverse motions of particles in the other beam. The betatron tune, the number of transverse oscillations a particle makes during one revolution of the machine, may change significantly due to the electromagnetic forces. The shift of the tunes is a function of the oscillation amplitude and this leads to a spread of betatron tune in each beam. When the tune spread is large enough to overlap resonance lines, the beam size increases and the particles in two beams can be lost, thereby limiting the maximum luminosity and shortening the luminosity lifetime. Two possible solutions exist for preventing the luminosity decay. One is to separate the beams at unwanted crossing points by either electrostatic separators[6] or using two separate rings[7]. These techniques can reduce the beam-beam effect, but usually at a very high cost.

The second, a new approach described in this dissertation, is to choose the optimum working point in the tune space in order to provide a larger resonance-free space that can accommodate the tune spread. The largest resonance-free space exists near an integer in tune space.[8] The disadvantage of this is that any integer is a very strong resonance line and it may cause beam loss and orbit distortion problems, so that accelerator physicists have always avoided choosing the working point near an integer. The experiments described in this dissertation are intended to investigate the benefits and difficulties associated with operating a hadron collider with betatron tunes near an integer. In particular, experiments have been performed to find a way to maintain a stable storage of two colliding beams near integer tune values when the tune shift is too large to be accommodated elsewhere in the tune space.

CHAPTER II

EFFECTS OF BEAM-BEAM INTERACTION

In a collider, two beams collide with each other. The electromagnetic force between the beams at each crossing point distorts the motion of the particles in each beam. These distortions and their consequences are called beam-beam interaction effects. In this chapter, the motion of a single beam in an accelerator will be discussed first. Following this, the electromagnetic force between two beams will be examined together with the tune shift and tune spread caused by this force.

2.1 Motion of a single beam in an accelerator

Storage rings are composed of sequences of magnetic elements. The sum of all magnetic elements, their strengths and placements, is called a "lattice". The motion of a particle in a lattice is described relative to the reference orbit corresponding to the reference momentum p_o. The periodic orbit which closes upon itself after one turn is called the closed orbit. If one keeps only the linear terms of the magnetic field around the reference orbit, the homogeneous equations of motion have the following form for the horizontal and the vertical motions:[9]

$$\frac{d^2x}{ds^2} + K_x(s)x = 0, \qquad (2-1)$$

$$\frac{d^2y}{ds^2} + K_y(s)y = 0. \qquad (2-2)$$

The variables x and y are, respectively, the horizontal and vertical deviations from the reference orbit, s is the distance along the reference orbit, and $K(s)$ is

a function of s defined by the lattice. For a ring with circumference C, $K(s)$ is periodic in s.

$$K(s+C) = K(s) \qquad (2-3)$$

In this case the corresponding homogeneous equations are known as Hill's equation. The focusing force is represented by $K(s)$. The motion is an oscillation about the reference orbit with an amplitude which depends on s. It is called betatron motion because it was first studied in betatrons.

The solution of the equations can be written in a pseudo-harmonic oscillation form introduced by Courant and Snyder.[10] The solution x and it's derivative $x' \equiv dx/ds$ can be written as

$$x = \sqrt{\epsilon_o \beta(s)} \cos \psi(s) \qquad (2-4)$$

$$x' = -\sqrt{\epsilon_o / \beta(s)} [\sin \psi(s) - \frac{\beta'}{2} \cos \psi(s)] \qquad (2-5)$$

with phase function

$$\psi(s) = \psi(s_o) + \int_{s_o}^{s} \frac{ds'}{\beta(s')} \qquad (2-6)$$

where ϵ_o and $\psi(0)$ are two constants given by the initial conditions. $\beta(s)$ is called the amplitude function or beta-function and it is periodic in s with the period C, $\beta(s+C) = \beta(s)$. It is the solution of the differential equation

$$\frac{1}{2}\beta\beta'' - \frac{1}{4} + K\beta^2 = 1. \qquad (2-7)$$

The number of betatron oscillations in one revolution is the tune ν,

$$\nu = \frac{1}{2\pi}\int_s^{s+C} \frac{ds'}{\beta(s')}. \qquad (2-8)$$

2.2 Beam-beam force

Particles circulating in a collider ring experience localized periodic kicks when crossing the opposing beam. Consider a head-on collision between two round Gaussian bunches which have length L with n particles per unit length and with a transverse charge density distribution[11]

$$\rho(r) = \frac{ne}{2\pi\sigma^2} e^{-r^2/2\sigma^2} \qquad (2-9)$$

where σ is the rms radial beam size and e is proton charge. The electromagnetic force on a test particle at radius r is

$$\begin{aligned}\vec{F} &= e(\vec{E} + \vec{v} \times \vec{B}) \\ &= e(E_r + \beta_r c B_\phi) \cdot \vec{r_o}\end{aligned} \qquad (2-10)$$

with $\vec{r_o}$, the unit vector in cylindrical coordinates (r, ϕ, z).

One can obtain the electric field E_r and magnetic field B_ϕ respectively from Gauss' theorem and Ampère's law

$$E_r = \frac{ne}{2\pi\varepsilon_v}\frac{1}{r}(1 - e^{-r^2/2\sigma^2}) \qquad (2-11)$$

$$B_\phi = \frac{ne\mu_v\beta_r c}{2\pi}\frac{1}{r}(1 - e^{-r^2/2\sigma^2}). \qquad (2-12)$$

Therefore

$$F_r = \pm\frac{ne^2}{2\pi\varepsilon_v}(1 + {\beta_r}^2)\frac{1}{r}(1 - e^{-r^2/2\sigma^2}) \qquad (2-13)$$

where the negative sign corresponds to oppositely charged particles and the positive sign corresponds to particles of the same charge. The angular kick $\Delta r'$ which a particle receives from the interaction force F_r is

$$\Delta r' = F_r\frac{L}{2\beta_r c}\cdot\frac{1}{e(B\rho)} \qquad (2-14)$$

where $B\rho$ is the rigidity of the particle.

In the case of proton-antiproton interactions such as in the Tevatron collider, the angular kick $\Delta x'$ corresponding to the beam-beam interaction is given by

$$\Delta r' = -\frac{Ne}{2\pi\epsilon_v \cdot \beta_r c \cdot (B\rho)} \cdot \frac{1}{r}(1 - e^{-r^2/2\sigma^2}) \qquad (2-15)$$

where $N = nL$ is the number of particles per bunch.

The angular kick $\Delta r'$ is plotted in Fig.1 for the proton-antiproton interaction as a function of the betatron amplitude of a test particle. The amplitude, when normalized to the rms beam size σ, can be divided into three regions:

$$\frac{r}{\sigma} \ll 1, \qquad \frac{r}{\sigma} \approx 1 \quad \text{and} \quad \frac{r}{\sigma} \gg 1.$$

Within the region $\frac{r}{\sigma} \ll 1$, using the expansion of $e^{-r^2/2\sigma^2}$, one obtains a kick $\Delta r'$ which is linear in r

$$\Delta r' \approx -\frac{Ne}{2\pi\epsilon_v \cdot \beta_r c \cdot B\rho}\frac{r}{2\sigma^2}. \qquad (2-16)$$

This is a quadrupole-like kick, because it is similar to a kick which a particle receives from a quadrupole magnet. In the Hill's equation, it corresponds to a change in the restoring force which alters the betatron tune. While a quadrupole magnet focuses in one direction and defocuses in the other, the $P\bar{P}$ force focuses

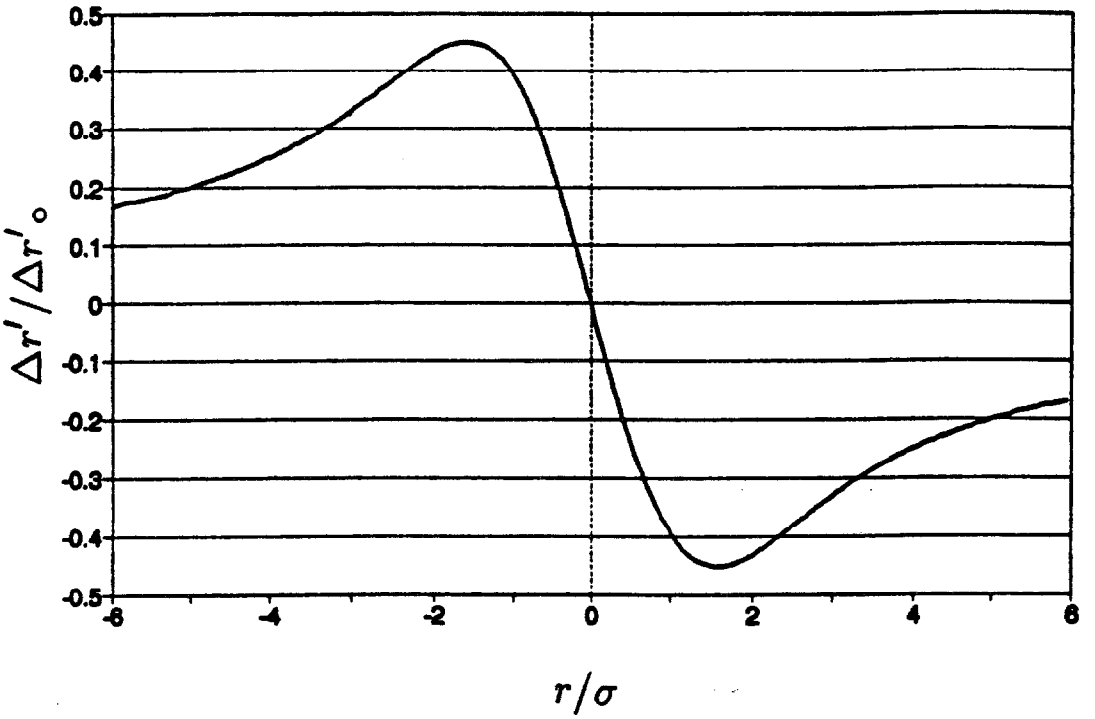

Figure 1. The angular kick $\Delta r'$ for the proton-antiproton interaction as a function of the betatron amplitude of a test particle. The amplitude is normalized to the *rms* beam size σ.

in both horizontal and vertical directions and, for small amplitudes, both tunes are increased corresponding to the beam-beam interaction.

For the region with $\frac{r}{\sigma} \approx 1$, the force is more complex and not linear in r. A particle in this region receives a kick from the beam-beam interaction force which will drive all of the even numbered resonances, because the potential due to the antisymmetric force (2-13) is an even function of x and y which can be expanded in an even-order series.

The kick due to long-range interaction, when $\frac{r}{\sigma} \gg 1$, varies slowly with r. It corresponds to a dipole-like kick.

2.3 Linear tune shift

For a small amplitude, $(\frac{r}{\sigma}) \ll 1$, the beam-beam kick is equivalent to what is given by a thin lens of focal length f

$$\frac{1}{f} = -\frac{\Delta x'}{x} \qquad (2-17)$$

and

$$\frac{1}{f} = -\frac{\Delta y'}{y}. \qquad (2-18)$$

From (2-16),

$$\begin{aligned} \frac{1}{f} &= \frac{Ne}{2\pi\varepsilon_v \cdot \beta_r c \cdot B\rho} \cdot \frac{1}{2\sigma^2} \\ &= \frac{Nr_p}{\sigma^2 {\beta_r}^2 \gamma_r} \end{aligned} \qquad (2-19)$$

where r_p is the classical proton radius

$$r_p = \frac{e^2}{4\pi\epsilon_v(m_pc^2)}.$$

The transformation through the beam-beam interaction in each transverse direction is described by the matrix

$$\begin{pmatrix} 1 & 0 \\ -\frac{1}{f} & 1 \end{pmatrix} \quad \text{or} \quad \begin{pmatrix} 1 & 0 \\ -k(s)ds & 1 \end{pmatrix} \tag{2-20}$$

where $k(s)$ is the focusing function due to the beam-beam interaction. To investigate the perturbation of the lattice function by this lens, we compute the perturbed one-turn transfer matrix

$$\begin{aligned} &\begin{pmatrix} \cos\mu + \alpha\sin\mu & \beta\sin\mu \\ -\gamma\sin\mu & \cos\mu - \alpha\sin\mu \end{pmatrix} \\ &= \begin{pmatrix} 1 & 0 \\ -k(s)ds & 1 \end{pmatrix} \begin{pmatrix} \cos\mu_o + \alpha_o\sin\mu_o & \beta_o\sin\mu_o \\ -\gamma_o\sin\mu_o & \cos\mu_o - \alpha_o\sin\mu_o \end{pmatrix} \end{aligned} \tag{2-21}$$

where α and γ are Courant-Snyder parameters and $\mu \equiv 2\pi\nu$ is the phase advance in one revolution.

Carrying out the multiplication and equating the trace of the matrix, we find

$$2\cos\mu = 2\cos\mu_o - (\beta_o \sin\mu_o)k(s)ds. \qquad (2-22)$$

Adding the contribution from all the crossings over the whole circumference, we obtain, in the lowest order in $k(s)$,

$$\Delta(\cos\mu) = \cos\mu - \cos\mu_o = -\frac{\sin\mu_o}{2}\int_0^C \beta_o(s)k(s)ds. \qquad (2-23)$$

The quantity

$$\xi = \frac{1}{4\pi}\int_0^C \beta_o(s)k(s)ds \qquad (2-24)$$

is known as the "linear tune shift" parameter of the beam-beam interaction. The linear tune shift is

$$\Delta\nu = \frac{\Delta\mu}{2\pi} \simeq -\frac{\Delta(\cos\mu)}{2\pi(\sin\mu_o)} = \xi. \qquad (2-25)$$

2.4 Tune spreads

The horizontal and vertical tune shifts $\Delta\nu$ are directly related to the slopes of the beam-beam forces, $\partial f/\partial x$ and $\partial f/\partial y$, at the position of the test particle.[12] As the slope is a function of the position, the tune shift of small-oscillation particles is ξ and the tune shift for large oscillation particles is smaller. The tune shift is the function of a position of the particles at the interaction point. Since

a beam contains a distribution of particles of various amplitudes, the position of each particle could be from 0 to amplitude and it ends up with a tune spread. Since the maximum slope of the beam-beam force $\partial f/\partial x$ and $\partial f/\partial y$ is at $x = 0$ and $y = 0$, the tune spread of the beam is equal to the amount of tune shift of small amplitude particles:

$$\textit{Tune spread} \leq |\xi|. \qquad (2-26)$$

2.5 Stability of linear motion

In the linear approximation, the motion of a particle is stable only if the absolute value of the trace of the one-turn transfer matrix is less than 2, that is

$$-1 \leq \cos\mu_o - 2\pi\xi \sin\mu_o \leq 1.$$

Considering the region of $0 < \mu_o < \pi$, one obtains the stable region in (μ, ξ) space:

$$-\frac{1}{2\pi}\tan(\mu_o/2) \leq \xi \leq \frac{1}{2\pi}\cot(\mu_o/2). \qquad (2-27)$$

In the region of $\pi < \mu_o < 2\pi$, one obtains the same result. Fig.2 shows the stable region in (μ, ξ) space.

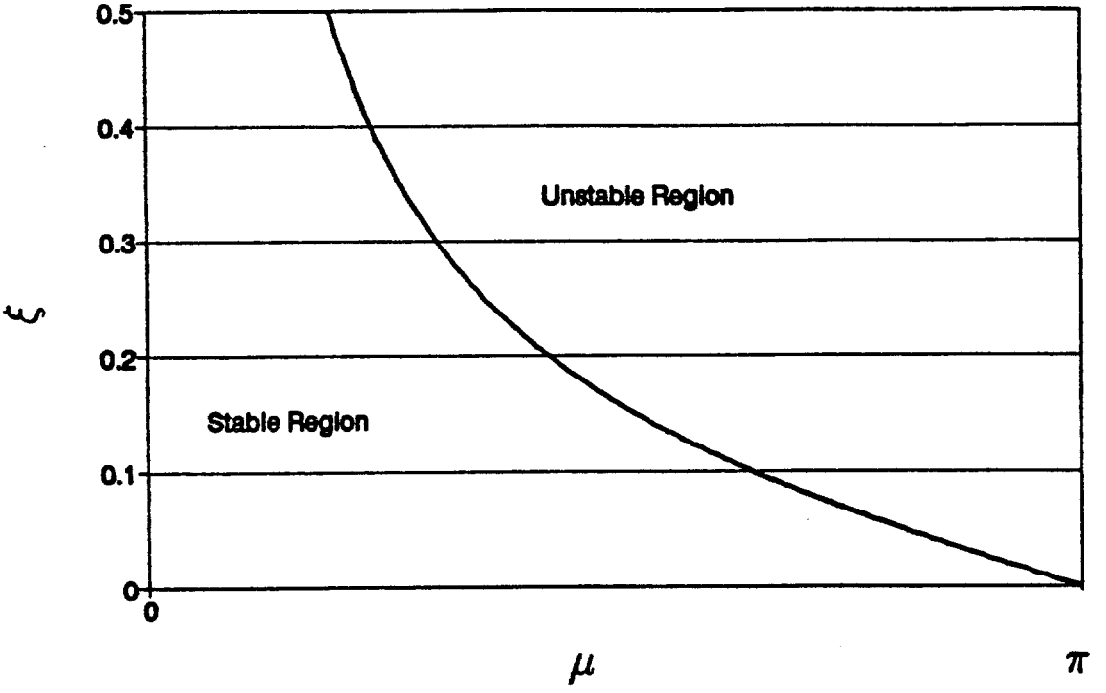

Figure 2. The stable region in (μ, ξ) space.

2.6 The width of the stopband

The expression (2-25) is the lowest order approximation and terms of second and higher orders in k are neglected. When $\sin\mu_o$ is near zero, that is, when the tune $\mu/2\pi$ is near an integer or a half-integer, the second order contributions must be considered. If there is a perturbation at s_1 and another at s_2, the one-turn matrix at s_1 is

$$\mathbf{M}(s_1) = \begin{pmatrix} 1 & 0 \\ -k(s_1)ds_1 & 1 \end{pmatrix} \mathbf{B} \begin{pmatrix} 1 & 0 \\ -k(s_2)ds_2 & 1 \end{pmatrix} \mathbf{A} \qquad (2-28)$$

where $\mathbf{A}$ is the matrix of the unperturbed system from s_1 to s_2, and $\mathbf{B}$ is the matrix from s_2 to $s_1 + C$. We have

$$\begin{aligned} \mathbf{M}(s_1) = \mathbf{M}_o(s_1) &- ((\mathbf{RBA})k(s_1)ds_1 \\ &- (\mathbf{BRA})k(s_2)ds_2 + (\mathbf{RBRA})k(s_1)k(s_2)ds_1ds_2 \end{aligned} \qquad (2-29)$$

where

$$\mathbf{R} = \begin{pmatrix} 0 & 0 \\ 1 & 0 \end{pmatrix}.$$

The trace of $\mathbf{M}(s_1)$ is

$$\begin{aligned} 2\cos\mu = 2\cos\mu_o &- (k_1\beta_1 ds_1 + k_2\beta_2 ds_2)\sin\mu_o \\ &+ B_{12}A_{12}k_1k_2ds_1ds_2 \end{aligned} \qquad (2-30)$$

with $B_{12} = \sqrt{\beta_1\beta_2}\sin(2\pi\nu_o + \psi_1 - \psi_2)$, $A_{12} = \sqrt{\beta_1\beta_2}\sin(\psi_2 - \psi_1)$. Then

$$\cos\mu - \cos\mu_o = -\frac{\sin\mu_o}{2}\int_0^C k(s)\beta(s)ds + \frac{1}{2}\int_0^C ds_1\int_{s_1}^C ds_2 k_1 k_2 \beta_1\beta_2 \sin[\nu_o(\phi_2 - \phi_1)]\sin[\mu_o - \nu_o(\phi_2 - \phi_1)]. \tag{2-31}$$

The width of linear resonance stopband is the width of the range of $\nu_o = \mu_o/2\pi$ over which the absolute trace of the perturbed one-turn matrix is bigger than 2. In (2-31), $\phi \equiv \psi/\nu$ is the normalized phase.

Consider the case where ν is nearly an integer:

$$\nu = p + \epsilon \tag{2-32}$$

with p an integer and $|\epsilon| \ll 1$, then to second order in ϵ

$$\sin\mu_o \approx 2\pi\epsilon; \quad \cos\mu_o \approx 1 - 2\pi^2\epsilon^2 \tag{2-33}$$

Neglecting terms of higher than the second order in ϵ and k, and replacing the integral over the triangular region by a half of the integral over the square region, we obtain, after some manipulation,

$$\cos\mu - 1 = -2\pi^2\epsilon^2 - \pi\epsilon I_0 + \frac{1}{8}(|\ I_{2p}\ |^2 - {I_0}^2), \tag{2-34}$$

where, for any n,

$$I_n = \int_0^C \beta(s)k(s)e^{-in\phi(s)}ds \qquad (2-35)$$

Solving for $\cos\mu - 1 = 0$, we have

$$\varepsilon = -\frac{I_0 \pm \mid I_{2p} \mid}{4\pi} \qquad (2-36)$$

so that the width of the stopband is

$$\delta\nu = \frac{\mid I_{2p} \mid}{2\pi} = \frac{1}{2\pi}\mid \int_0^C \beta(s)k(s)e^{2ip\phi(s)}ds \mid. \qquad (2-37)$$

Since $k(s)$ could be induced by beam-beam interactions or could be an error in quadrupole strength, this expressions for $\delta\nu$ is general when the unperturbed tune is close to an integer.

Similarly, the width of the half integer stopband is

$$\delta\nu = \frac{\mid I_{2p+1} \mid}{2\pi} = \frac{1}{2\pi}\mid \int_0^C \beta(s)k(s)e^{2i(p+1)\phi(s)}ds \mid. \qquad (2-38)$$

This expression for $\delta\nu$ should be valid for either horizontal or vertical direction if there is no coupling between the two directions. Near an integer, many nonlinear resonances exist but only the linear and uncoupled resonances are considered in the discussion since the linear resonances are in general more serious than nonlinear resonances near integer or half integer tunes.

CHAPTER III

WORKING POINT IN TUNE SPACE

3.1 Working point in tune space

The betatron tunes ν_h and ν_v are defined to be the number of transverse oscillations per revolution while the synchrotron tune ν_s is defined as the number of longitudinal (*i.e.*, momentum) oscillations per revolution. It follows that

$$\nu_h = f_h / f_{rev} \tag{3-1}$$

$$\nu_v = f_v / f_{rev} \tag{3-2}$$

$$\nu_s = f_s / f_{rev} \tag{3-3}$$

These three tunes define a three dimensional tune space where a collider working point (ν_h, ν_v, ν_s) is a point in the three dimensional tune space. However, only the transverse motion of beams is studied in this work and a working point always refers to a point (ν_h, ν_v) in the two dimensional sub-tune space.

To achieve high luminosity and luminosity lifetime, we must keep particles away from resonances so that the motion of betatron oscillations of particles is stable.

3.2 Resonance

In general, resonances leading to beam instabilities are of the form, [9] [10] [13]

$$m\nu_h + n\nu_v = p, \qquad (3-4)$$

where m, n and p are all integers. The sum of $|m|$ and $|n|$:

$$|m| + |n|$$

is called the order of the resonance. If m and n are opposite in sign, the resulting motions are coupled but they remain bounded. The order of the resonance is related to the order of the magnetic multipole field component which drives the resonance. For examples, 2nd-order resonances are driven by the quadrupole component and 3rd-order resonances are driven by the sextupole component.[9] [10] [13]

3.3 Tune diagrams

It is helpful to use a tune diagram, ν_h *vs.* ν_v plot with resonance lines, to analyze a working point. A tune diagram is usually plotted from integers (k, l) to $(k+1, l+1)$ since the fractional parts of the tunes determine the distance to the resonance condition. Fig.3 is a typical tune diagram with resonance lines up to 5th order.

In the tune diagram, one can choose a point to avoid resonance lines up to any specified orders. However, one must consider a resonance free area for a working point, because in a collider the tunes of all particles in a beam are not identical. As described in chapter II, beam-beam interaction causes a tune spread. Tune spread is also produced by the chromatic nature of the quadrupole focusing. The tune spread due to chromaticity ξ is given by

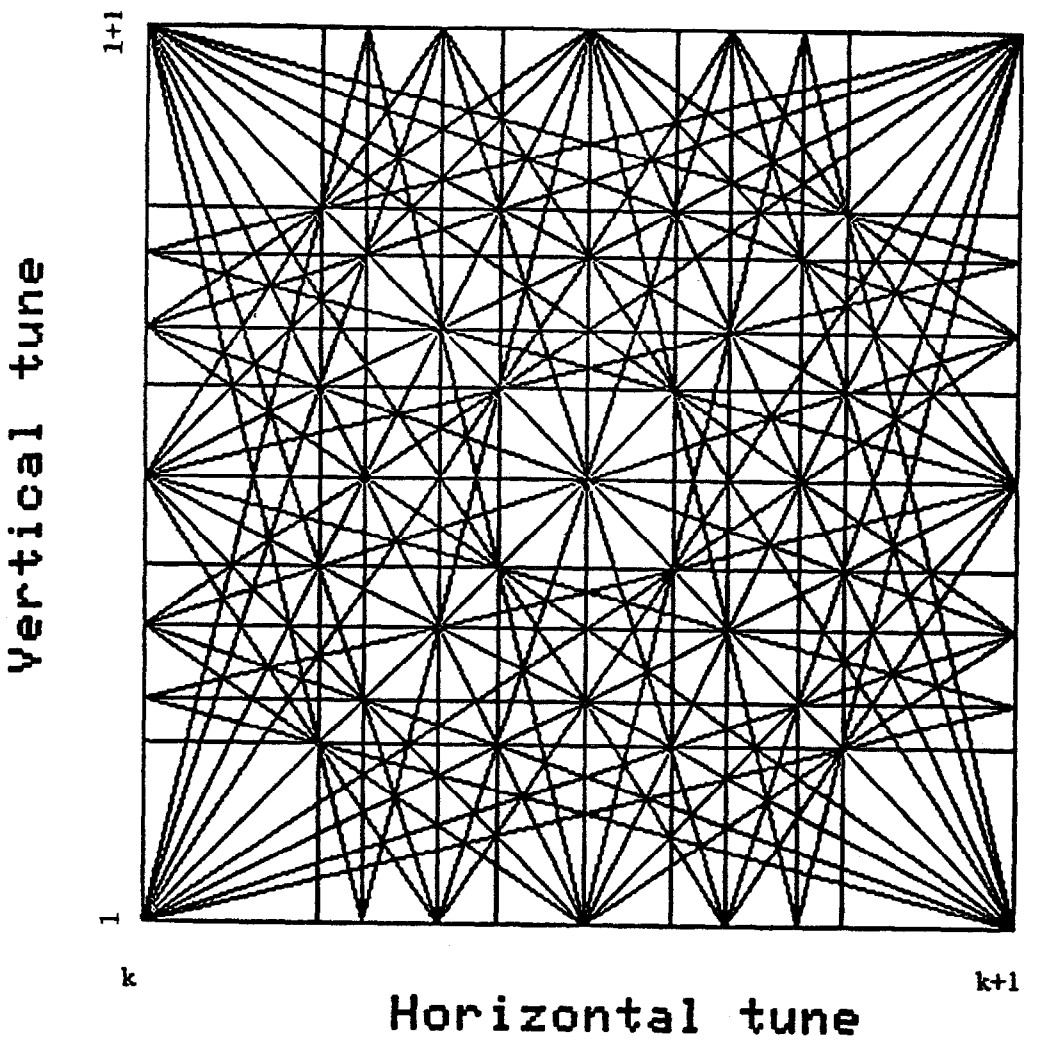

Figure 3. A two-dimensional tune diagram with resonance lines up to 5th order. k and l are integers.

$$\Delta\nu = \xi\frac{\Delta p}{p} \qquad (3-5)$$

where $\frac{\Delta p}{p}$ is the beam momentum spread. Beam-beam interactions lead to a tune spread of

$$\Delta\nu = N_B \cdot \frac{Nr_p\beta}{4\pi\sigma^2\gamma} = N_B \cdot \frac{Nr_p m_p \beta_r}{4\pi\epsilon_N} \qquad (3-6)$$

where N_B is the number of bunches in the ring and r_p is the classical proton radius.

For the Tevatron collider, the typical value of ξ is 3 and the *rms* momentum spread is 1.5×10^{-4} at 900 GeV. Thus the tune spread due to this momentum spread is approximately 5×10^{-4}.

The beam-beam tune spread of the antiproton beam for the 1989-1990 collider operation was 0.02 with 6 proton bunches. The working point was $(19.405, 19.41)$ as shown in Fig.4. It lies between the fifth-order and seventh-order resonance lines. The separation between these resonances is 0.028.

As higher luminosity is required, stores with 36 proton bunches (with 36 antiproton bunches) are expected. With the same proton bunch parameters, the beam-beam tune spread will then be 0.12. A larger resonance free area will be needed to accommodate this spread.

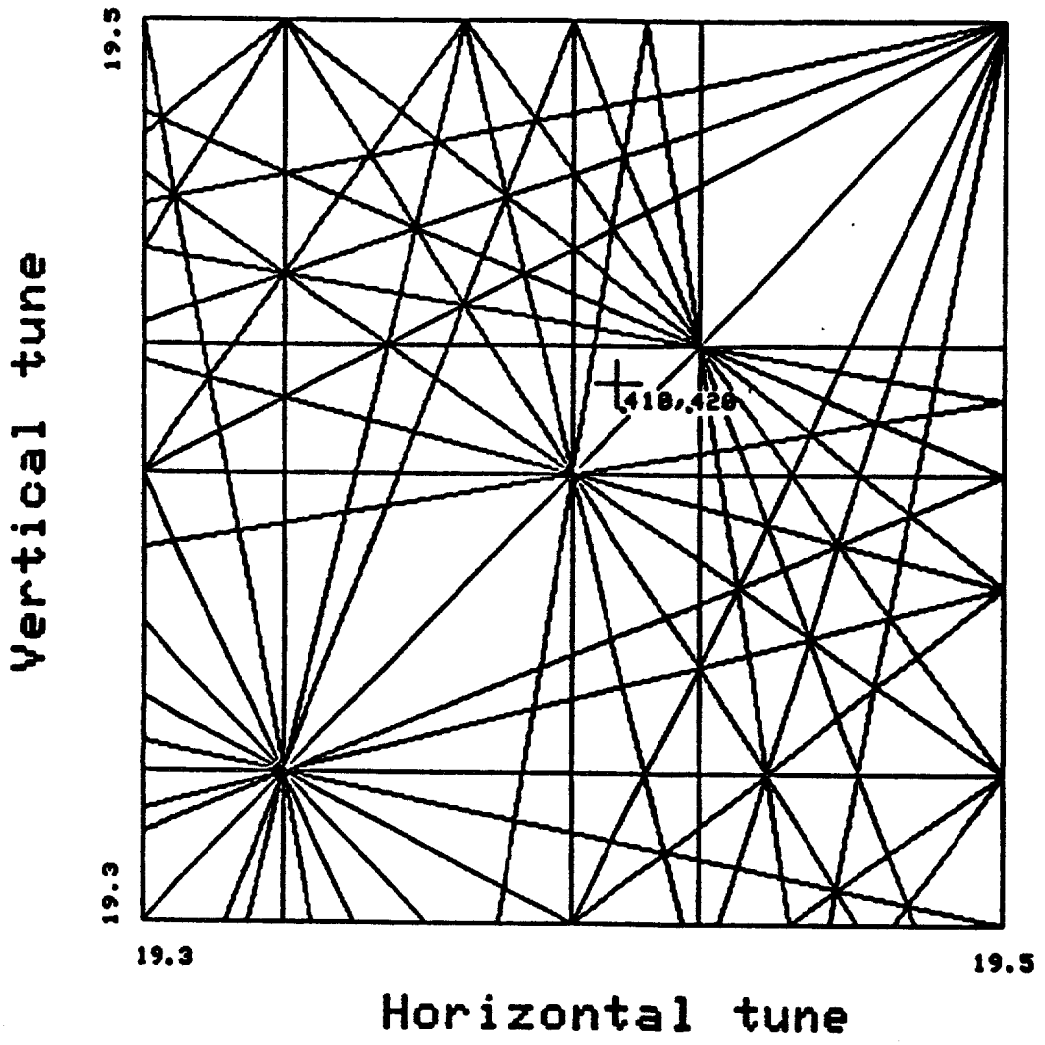

Figure 4. A tune diagram with resonance lines up to 7th order and the working point for 1989-1990 collider operation.

3.4 Integer *vs.* half integer values

The largest resonance free area is found near an integer. One can show that the Nth-order resonance line is separated from an integer by $\frac{1}{N}$. For example, the 7th order resonance is separated from an integer by 1/7 =0.143. Fig.5 is a tune diagram near 19 plotted from 19.0 to 19.2 for both ν_h and ν_v with resonance lines up to the 7th order. The 7th order resonance line is near 19.14.

Consider δ_{int}, the width of the stopband of an integer resonance, and δN, the Nth-order resonance width. One may conclude that, near an integer, the resonance free area is

$$\frac{1}{N} - \frac{1}{2}\delta_{int} - \frac{1}{2}\delta_N \qquad (3-7)$$

if the Nth-order resonance is assumed to be the lowest order to be avoided. Near a half integer, the separation between the Nth order resonance line and the half integer line is given by

$\frac{1}{N}$ when N is an even number

$\frac{1}{2N}$ when N is an odd number.

Fig.4 is a tune diagram plotted from 19.3 to 19.5 for both ν_h and ν_v with resonance lines up to 7th order. Comparing the tune diagram near 19.0 with that near 19.5, one can see that the distance to even order resonances is the same in

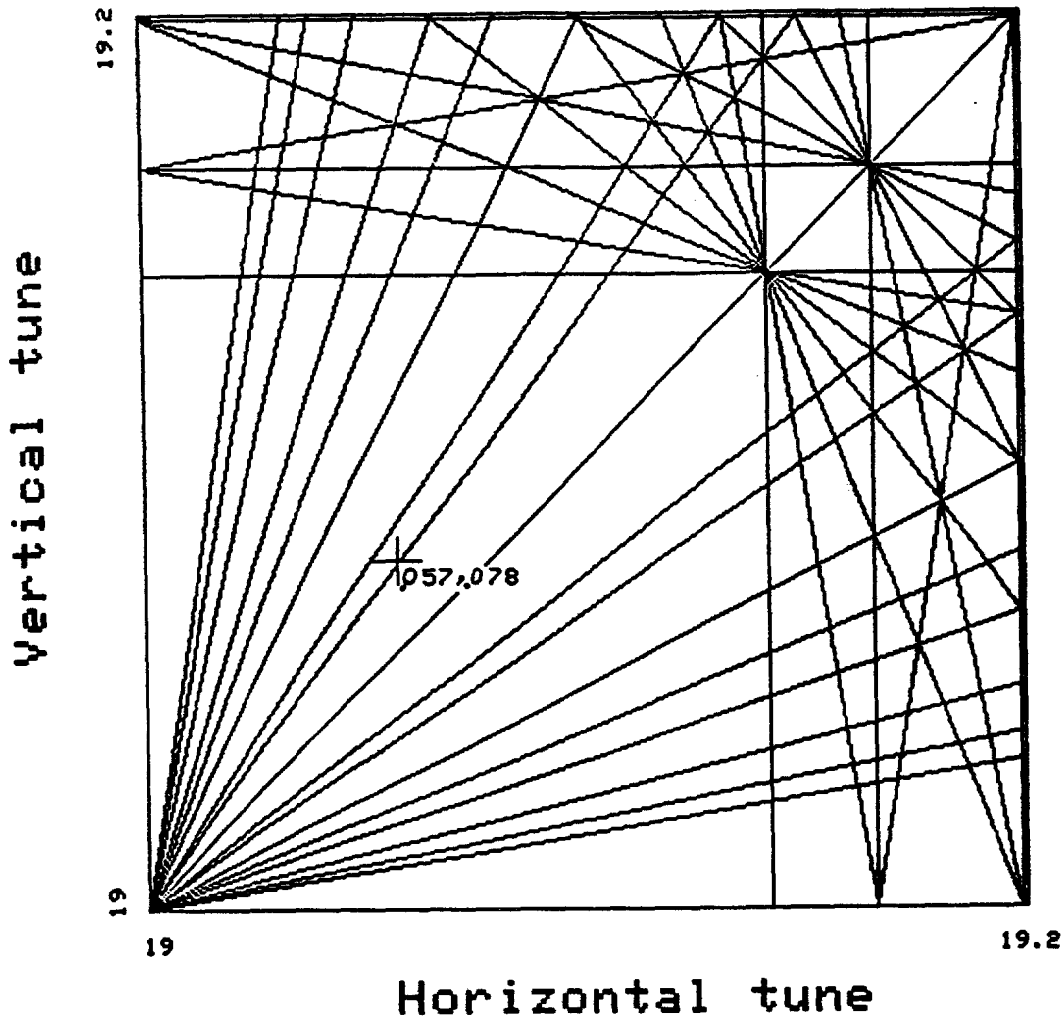

Figure 5. A tune diagram near 19.0 with resonance lines up to 7th order.

two cases while, for the odd order resonances, the distance is twice as large near 19.0.

Although the beam-beam force described in chapter II is an odd function of x, which means that the force drives the even order resonances only, the real beam in the Tevatron collider is not completely symmetric and the beam-beam force includes all of the odd and even terms and drives all the resonances. In the 1989-1990 Tevatron collider run, large antiproton beam losses were observed on the 5th and 7th order resonances near 19.5.[14] A working point near an integer is preferred for the Tevatron collider over a point near the half integer because of the reduced density of odd-order resonance lines, which are known to be important.

Considering these effects, we chose to investigate the region from 19.05 to 19.08 for the working point which has a resonance free space of 0.09 to 0.06 (up to the 7th order) to accommodate the beam-beam tune spread.

CHAPTER IV

MEASUREMENT TECHNIQUE

The measurement technique used for the experiments which are covered in chapters V, VI, VII, are briefly described in this chapter.

4.1 Beam intensity

The device installed in the Tevatron to measure the beam intensity is a resistive wall pickup which is a ceramic insert in the conductive vacuum tube. The signal is picked up on the resistors that bridge the ceramic insert. See Fig.6.

A modulated beam current I_b is accompanied by a "wall current" I_w which is induced in the wall of the vacuum tube. I_w has the approximately equal magnitude but opposite direction of I_b. As a result, the voltage induced on the resistors measures the beam current. The time integral of the current is a measure of the intensity. A pickup of this type has a bandwidth of several GHz giving a longitudinal profile of the beam with a resolution of some 100 ps. In Fig.7 the measured bunch length is approximately 6 ns.

4.2 Closed orbit

The closed orbit is measured with beam position monitors (BPM) which are more or less uniformly distributed around the Tevatron ring. There are 216 BPMs in all, 108 for vertical and 108 for horizontal position measurements. The data from the BPMs give the vertical and horizontal positions of the closed orbit. Fig.8 is an example of the closed orbit display available in the control room.

A BPM is a pair of stripline pickups as shown in Fig.9. As the beam passes between the two striplines, electromagnetic fields induce voltage across the resistors which is transmitted along the coaxial cables. The relative strengths of the signals on the two cables is used to determine the beam position.

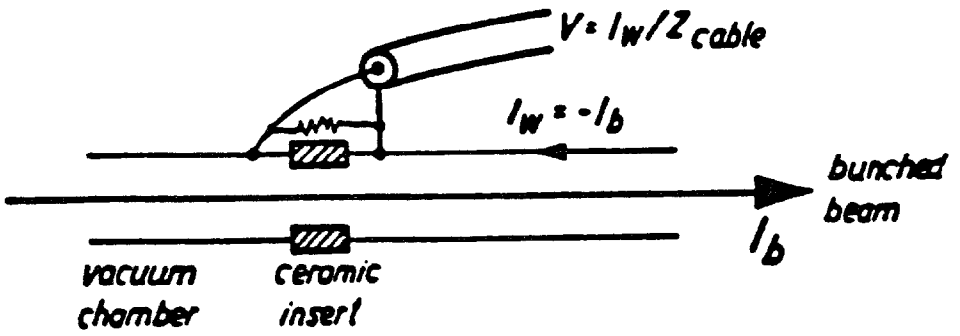

Figure 6. A resistive wall beam intensity pickup

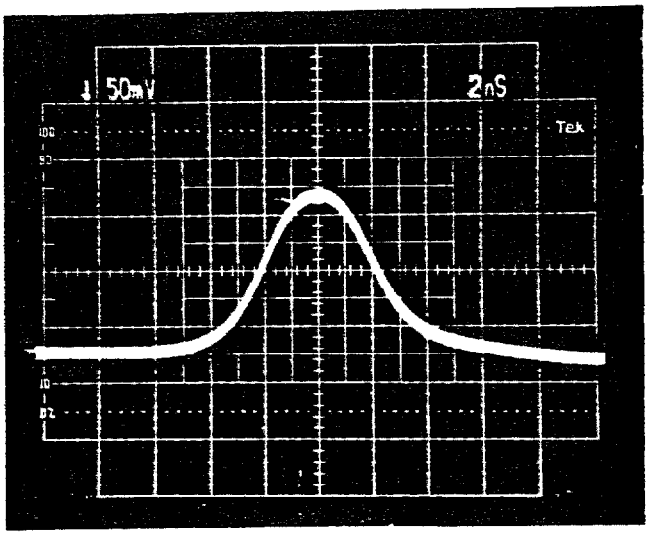

Figure 7. A typical beam intensity measurement

Vertical scale is $50mV/div.$ and horizontal scale is $2ns/div.$

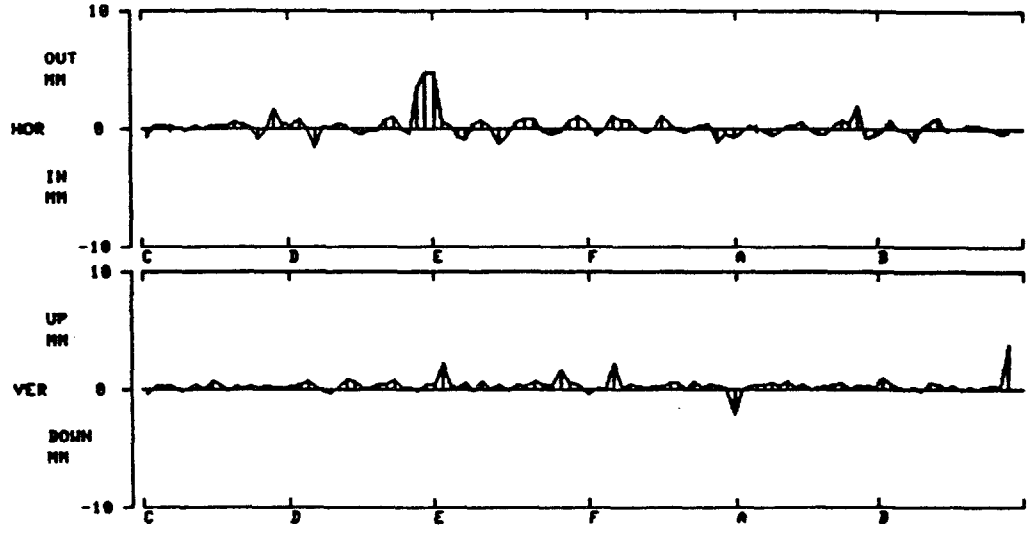

Figure 8. A typical closed orbit measurement in Tevatron

The circumference of the Tevatron is about $6.28km$ divided into 6 sectors.

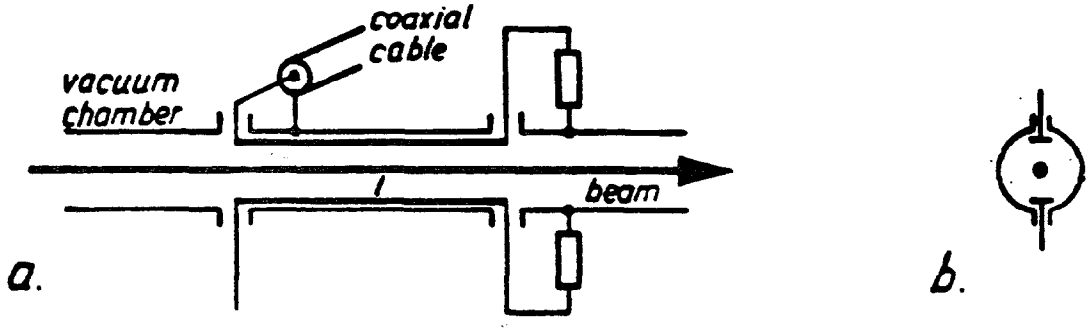

Figure 9. A stripline pickup beam position monitor and its cross section with two strips

4.3 Tunes

4.3.1 Betatron tune measurement.

The betatron tune is the number of transverse oscillations the beam makes about the closed orbit during one revolution in an accelerator. The tune is basically a property of the machine rather than of the beam, although it may depend on the beam intensity

A straight-forward way to measure the tune is to excite a bunch of particles to perform a coherent oscillation and measure the position of the beam center at all pickups around the ring for one turn. Subtracting the previously measured closed orbit from these readings and then normalizing to the square root of the betatron function, one obtains a sinusoidal function of betatron phase. The frequency of the curve is the full value of tune. This is a convenient way to measure the integer part of the tune and to see whether the tune is below or above half integer, but the fractional part can not be found so reliably in this method.

Usually, the accurate value of the fractional part is obtained by observing the signal from a single pickup which records the position of the beam for many revolutions. By Fourier transform, one can obtain an accurate fractional part of the tune value. For example, the dots in Fig.10 show the transverse position of a bunch on ten successive turns. One may draw a sinusoidal curve through them to obtain the curve labeled 0.41. However, other sinusoidal curves with other frequencies also pass through the same data points. In Fig.10, the curves labeled -0.59 and 1.41 are such examples. In general, possible frequencies are

$$f_m = (m \pm \nu) f_{rev} \qquad (4-1)$$

where f_{rev} is the revolution frequency and m is any integer.

A system to measure tunes in the Tevatron is shown in Fig.11. A sensitive detector resonant at 22 GHz picks up the beam position. After a bandpass filter, a frequency convertor converts the signals to audio frequency. These signals are transmitted to the main control room where a spectrum analyzer performs a Fast Fourier Transform(FFT).

A tune measurement of the Tevatron stored beam with tune near 19 is shown in Fig.12.

4.3.2 Tune control.

Control of the betatron tunes for the Tevatron is done by changing the strength of two circuits of quadrupole correction magnets. The magnets in one circuit are near the horizontally focusing main quadrupoles and primarily change the horizontal tune. The magnets in the other circuit are near vertically focusing main quadrupoles and primarily control the vertical tune.

The change in tune by a single quadrupole, $\delta\nu$, is given by Eq (2-22) or approximately given by its linear form:

$$\delta\nu = \frac{1}{4\pi}\frac{\beta_i \delta[B'l]_i}{B\rho} \qquad (4-2)$$

where $\delta[B'l]_i$ is the change in the integrated quadrupole strength, $B\rho$ is the magnetic rigidity of the beam and β_i is the beta function at the quadrupole location.[10][13]

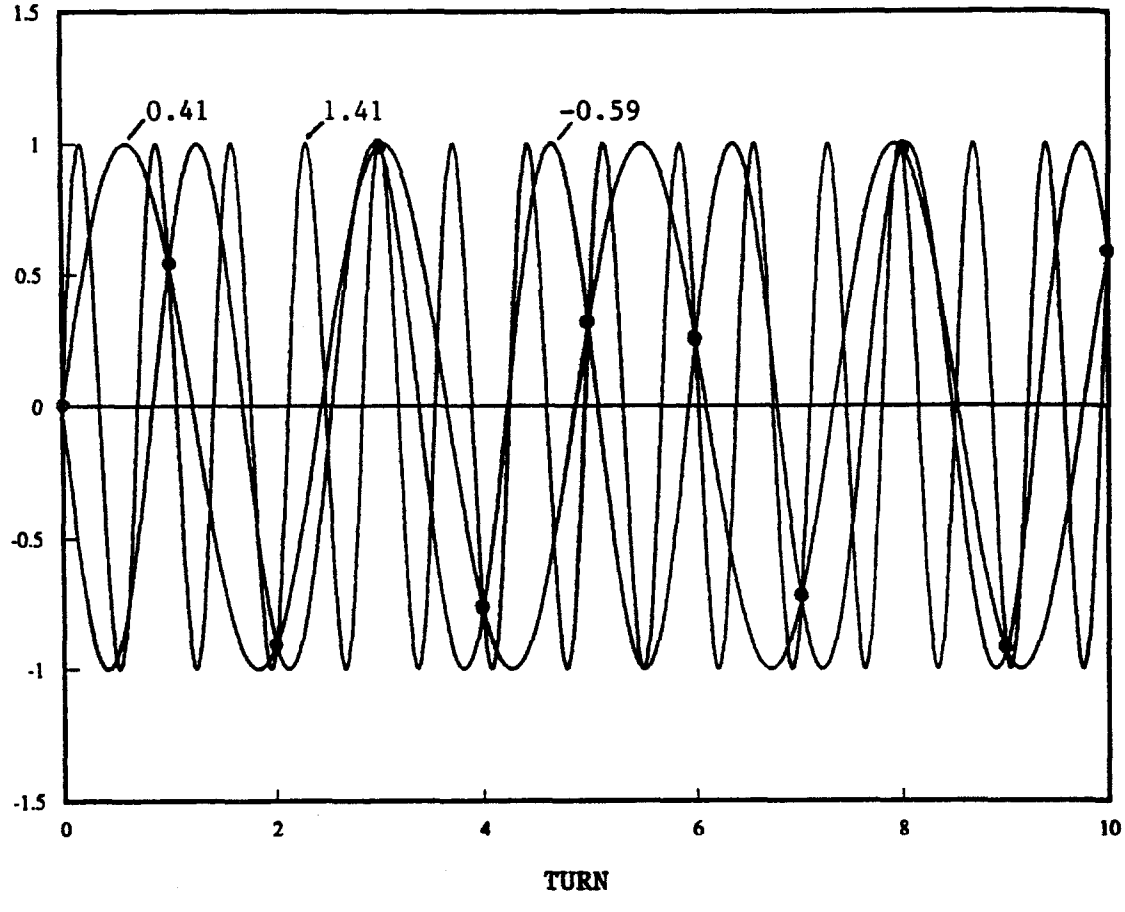

Figure 10. Beam position on ten successive turns and the three lowest frequency fits.

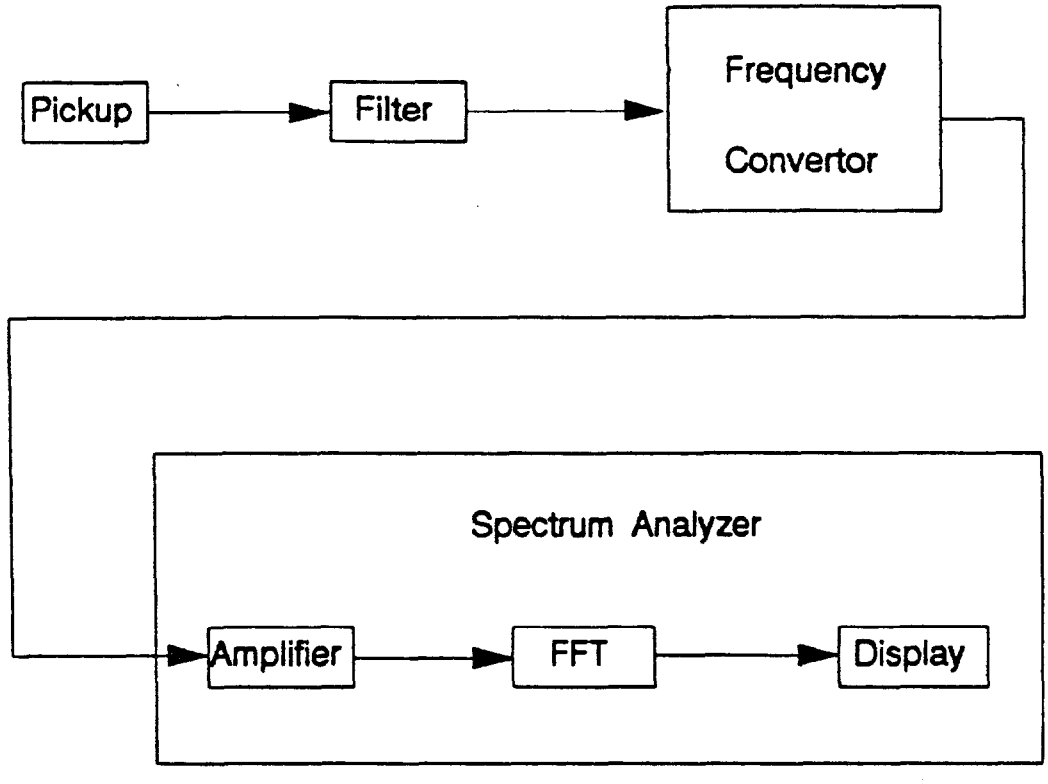

Figure 11. A block diagram of tune measurement system at Fermilab

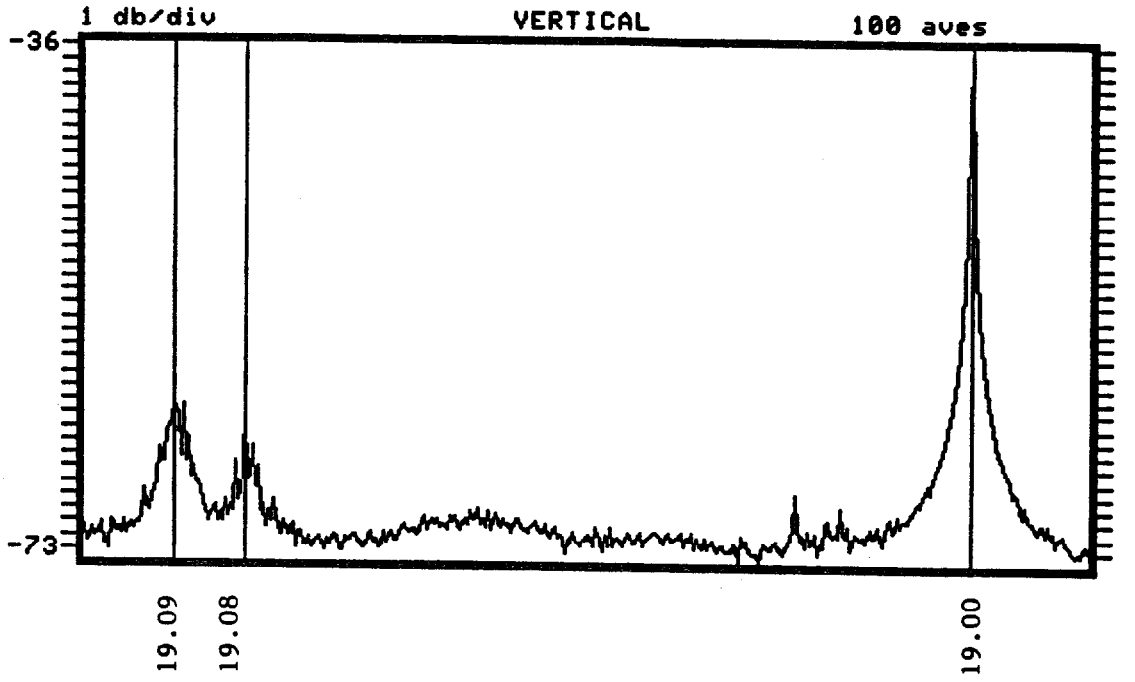

Figure 12. A tune measurement of the Tevatron stored beam with tune near 19. The right peak is the revolution signal and the left two peaks are horizontal and vertical tune signals. Measured fractional parts of horizontal and vertical tune are 0.08 and 0.09

4.4 Beta function

Measurement of the beta function at one location can be made by varying the strength of the quadrupole magnet at that location. This is clear from the relation given in Eq (4-2). In order to interpret betas in horizontal and vertical directions in an unambiguous manner, any existing linear coupling of two directions must be minimized.

Plotting $\delta\nu$ as a function of $\delta(B'l)$, one obtains the beta function at that location from the slope of the curve. Fig.13 is an example of a beta function measurement at the location (F34)in the Tevatron ring. In principle, one can measure the beta function wherever the strength of a quadrupole at that location can be varied. However, only a few quadrupoles can be independently controlled in the Tevatron and the beta function can be measured at these locations only. One way to check the measured beta function along an entire machine is by computing the beam optics. Computer codes called SYNCH and TEVLAT were used to compute the beta function and other parameters of synchrotrons. By comparing the beta functions computed from SYNCH and TEVLAT with measured beta function at several locations, one can estimate the reliability of the calculated values.

Fig.14 shows the measured and calculated values of beta functions for the Tevatron 150 GeV lattice.[15]

4.5 Transverse emittance

4.5.1 Beam size measurement.

A flying wire scanner, a fast moving wire crossing the circulating beam, is used to measure the beam size in some hadron storage rings. A speed of $20m/sec$ has been achieved with a $25\mu m$ diameter carbon wire. When the wire is crossing

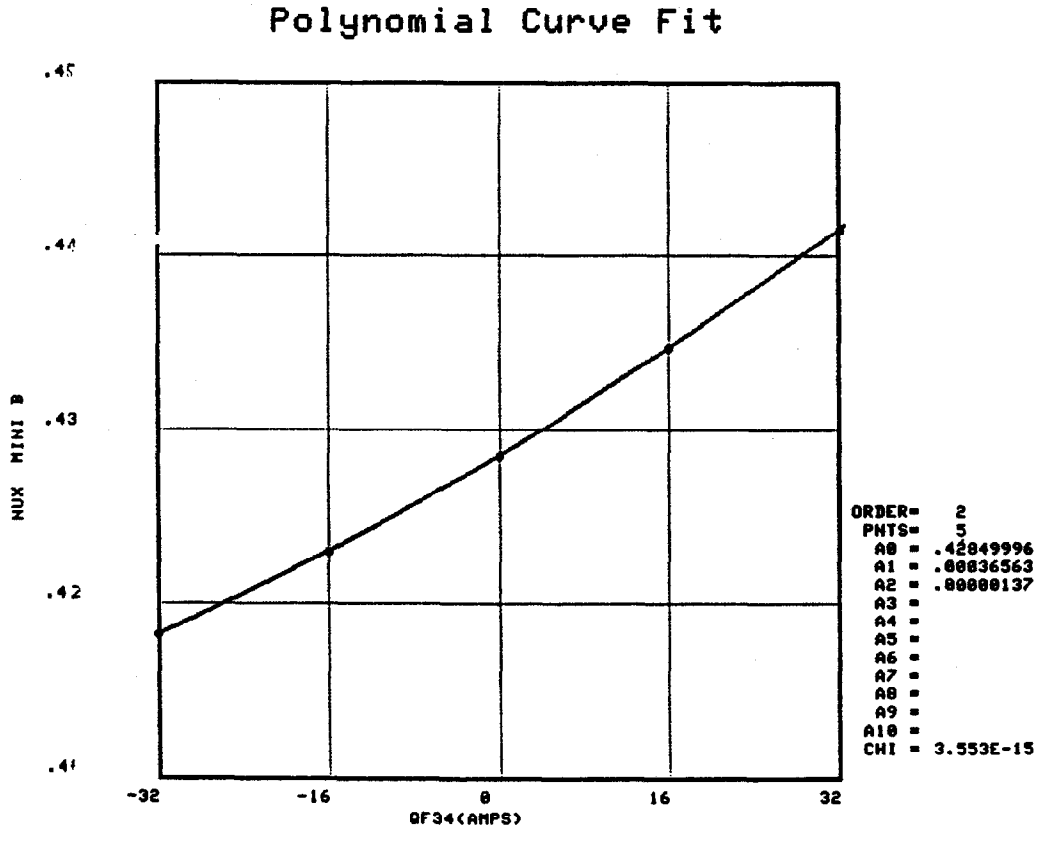

Figure 13. A beta function measurement at the location (F34) in the Tevatron ring by varying the strength of the quadrupole magnet at that location. The fitting coefficients of the polynomial series are shown on the right side of the figure,

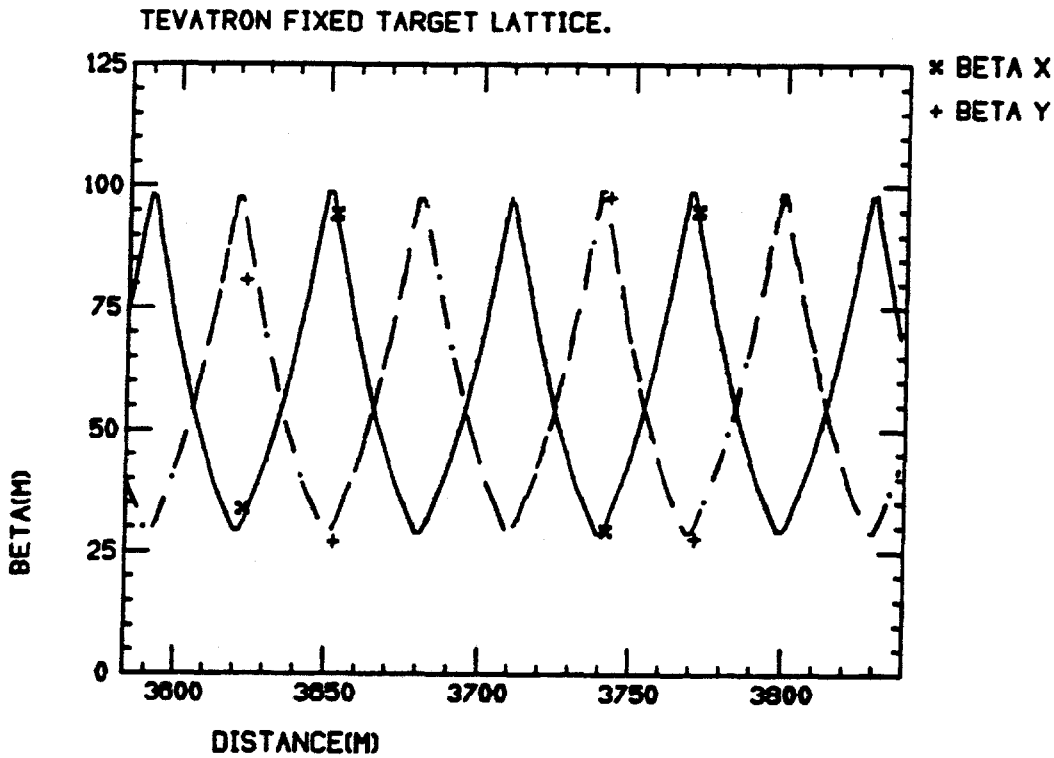

Figure 14. Measured and calculated values of beta functions for the Tevatron 150 GeV lattice. The points are measured values.

the beam, charged particles are produced from nuclear collisions with the carbon wire. A combination of a scintillator and a photomultiplier is used to measure the intensity of the charged secondaries and the beam transverse profile is obtained by plotting the photomultiplier circuit output as a function of the digitized wire position. A transverse profile of a beam measured by the flying wire is shown in Fig.15. The beam size σ is defined as the rms of the beam profile. The emittance and momentum spread of the beam are obtained through measurements of beam size.

4.5.2 Emittance.

Beam size δ, transverse emittance ϵ and the momentum spread $(\Delta p/p)$ in Gaussian distribution are related as follows:

$$\sigma^2 = \epsilon\beta + (\frac{\Delta p}{p}D)^2 \qquad (4-3)$$

where β is the local beta function and D is the local momentum dispersion function calculated by SYNCH. The momentum dispersion function can be obtained by measuring the closed orbit while varying the the frequency of acceleration voltage.

Once the beam sizes are measured, the emittances are calculated from the relation (4-3). In the horizontal plane, wires are needed at two different positions in order to find the emittance and the momentum spread separately,. In the vertical plane, the momentum dispersion function should be zero, since there is no bending in the vertical plane. Only one wire is required to find the vertical emittance of the beam.

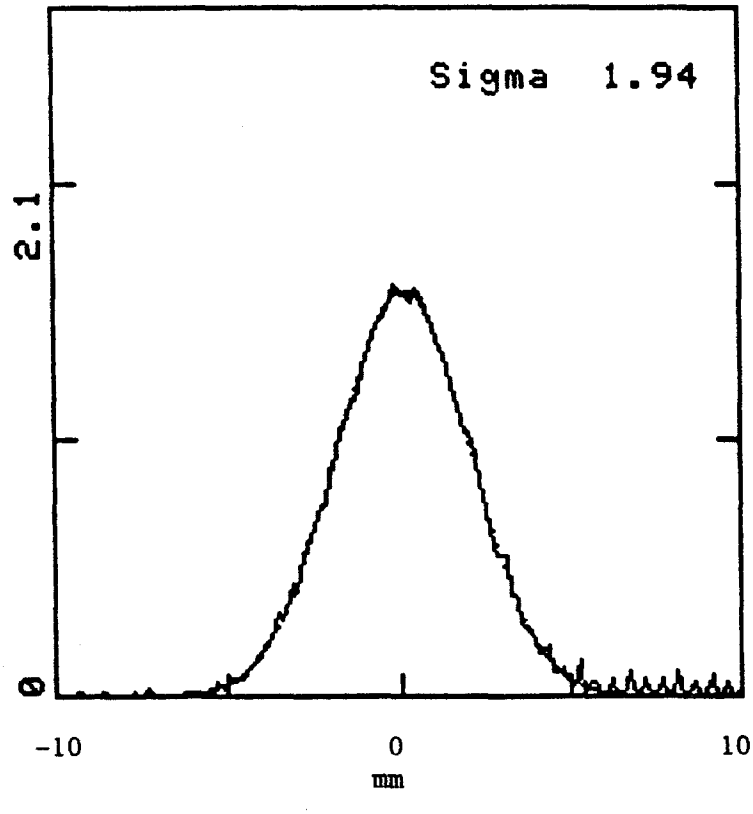

Figure 15. The horizontal profile of beam near tune of 19 is measured by the flying wire. The calculated rms size of the beam is 1.9 *mm*.

4.6 Luminosity

Luminosity $\mathcal{L}$ can be calculated from the measured beam parameters,

$$\mathcal{L} = \frac{N_p N_{\bar{p}} N_B f_{rev}}{4\pi\sigma_x\sigma_y} \qquad (4-4)$$

where N_p is the number of protons per bunch, $N_{\bar{p}}$ is the number of antiprotons per bunch, N_B is the number of bunches per beam (usually numbers of proton and antiproton bunches are the same), f_{rev} is the revolution frequency, and σ_x and σ_y are the rms beam size in the horizontal and vertical planes, respectively, at the interaction point (IP). The beam sizes are calculated from the measured ϵ and $\frac{\Delta p}{p}$ using calculated values of β and D at the IP. In the 1989-1990 Tevatron collider run, the typical measured luminosity was $1. \times 10^{34}\ m^{-2}s^{-1}$.

The luminosity can also be calculated from the interaction rate as measured from scintillation counters surrounding the IP, where $R = \mathcal{L}\sigma_{tot}$. R is the rate, and σ_{tot} is the part of the nuclear cross-section corresponding to the solid angle defined by the scintillation counters. The measured luminosity in the same run by this method is about 10% less than the other one.

CHAPTER V

EXPERIMENTS I & II

CONTROL OF THE CLOSED ORBITS

NEAR INTEGER TUNES

5.1 The control of the closed orbit

The ideal closed orbit should be in the middle of the available aperture. Orbit distortion near integer tunes is a serious problem in any synchrotrons for the following reason.

The closed orbit distortion at position s in a ring due to the error in the integrated magnetic field of the kth dipole or misaligned quadrupole is

$$x(s) = \frac{\sqrt{\beta(s)\beta_k}}{2\sin(\pi\nu)} \frac{\delta(Bl)_k}{B\rho} cos[\nu\pi - |\psi(s) - \psi_k|] \qquad (5-1)$$

where β_k and ψ_k are the betatron amplitude and phase, $\delta(Bl)_k$ is the integrated dipole field error and $\frac{\delta(Bl)_k}{B\rho}$ is the resulting kick causing the closed orbit distortion, all at position k. When the tune ν is near an integer, the factor $1/\sin(\pi\nu)$ is so large that a small dipole error $\delta(Bl)_k$ may lead to significant closed orbit distortions. Fig. 16 shows this factor $1/\sin(\pi\nu)$ as a function of the fractional part of ν. One can minimize the closed orbit distortion by using an algorithm for finding the correction dipole settings. We have used the 3-bump algorithm.

Consider a particle travelling on the ideal design orbit. Suppose that at $s = s_1$, it is kicked by a dipole such that it experiences an angular deflection θ_1. At $s = s_2$ and s_3, it is again kicked by dipoles and experiences angular deflections, θ_2 and θ_3, respectively as shown in Fig. 17. In order for the particle, which is on the design orbit at $s \leq s_1$, to end up again on the design orbit at $s \geq s_3$, we must have

$$\theta_2 = \theta_1 \sqrt{\frac{\beta_1}{\beta_2}} \frac{\sin(\psi_3 - \psi_1)}{\sin(\psi_3 - \psi_2)} \qquad (5-2)$$

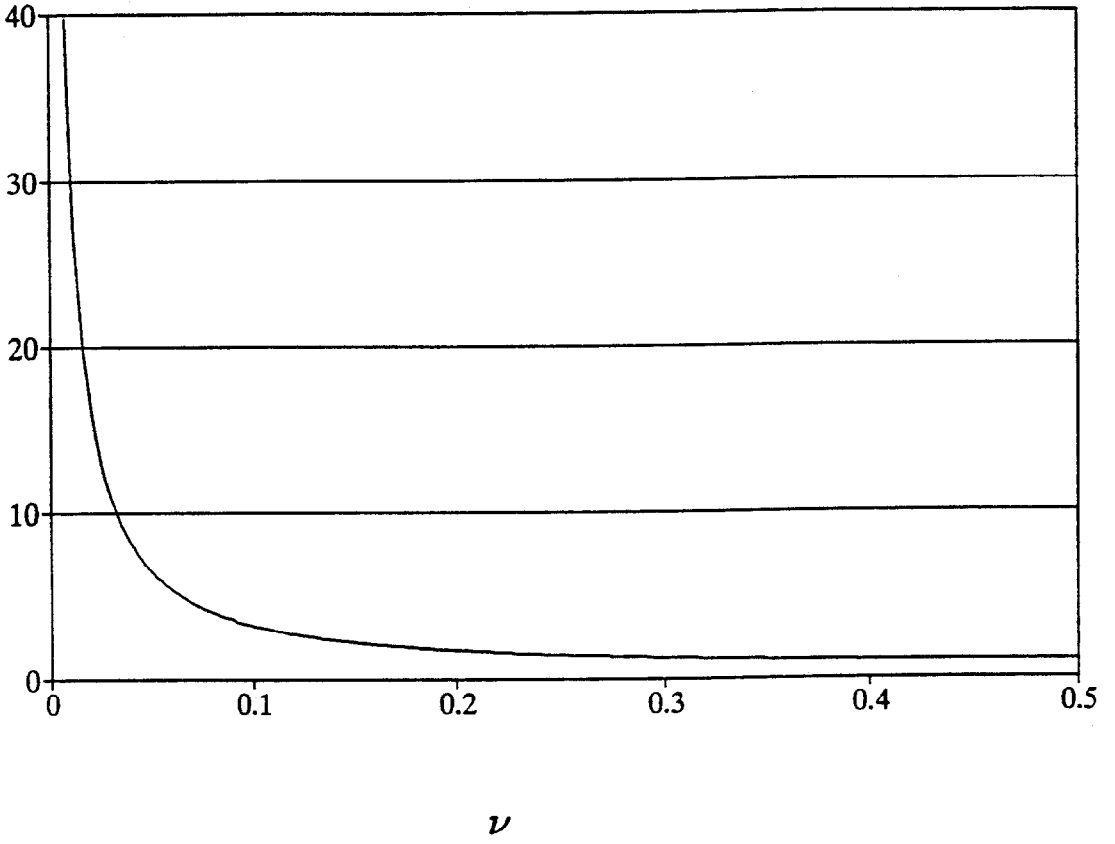

Figure 16. The factor of $1/\sin(\pi\nu)$

and

$$\theta_3 = \theta_1 \sqrt{\frac{\beta_1}{\beta_3}} \frac{\sin(\psi_2 - \psi_1)}{\sin(\psi_3 - \psi_2)}. \qquad (5-3)$$

This is called a "localized three-bump".

The important property of a localized three-bump is that any closed orbit deviation at s_2 can be created or, equivalently, any known orbit distortion at s_2 can be corrected without changing the positions outside the bump region, $s_1 < s < s_3$. The correction of the orbit distortion in the whole ring is achieved with the three-bump algorithm by stepping through each position measurement at the Beam Position Monitor (BPM) and adjusting the setting of three closest correction dipoles such that the corrected closed orbit would move to a desired position everywhere. This method works well when there is a BPM at each correction dipole position, as in the Tevatron.

There are 108 BPMs and 108 correction dipole magnets in each transverse direction to control the Tevatron orbit as described in chapter III. An on-line computer program reads the BPMs and uses the 3-bump algorithm to calculate the required correction dipole settings. Necessary machine parameters such as βs and ψs are stored in the program. Fig. 18 shows the BPM reading of the corrected closed orbit of the Tevatron when the beam is stored for collisions at a tune of 19.05. The rms distortion is less than $1mm$, which is about the same order as the distortion at the standard tune value of 19.4.

There was a concern that, near integer tune values, there might be an excessive sensitivity of the orbit distortion on the magnet power supply drifts. Experience showed, however, that the orbit was stable for several hours, with no corrections required after the initial adjustment.

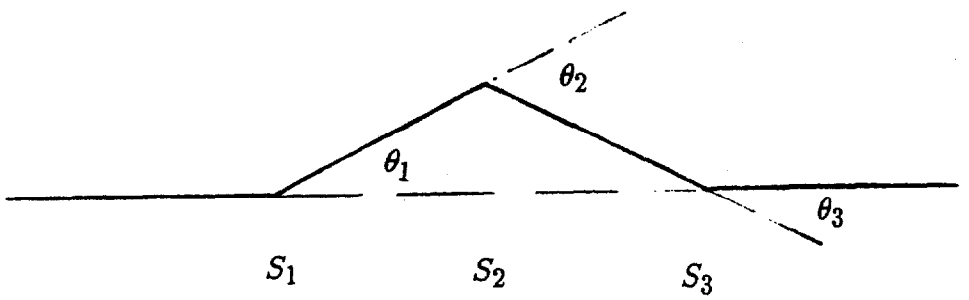

Figure 17. Three-bump-correction

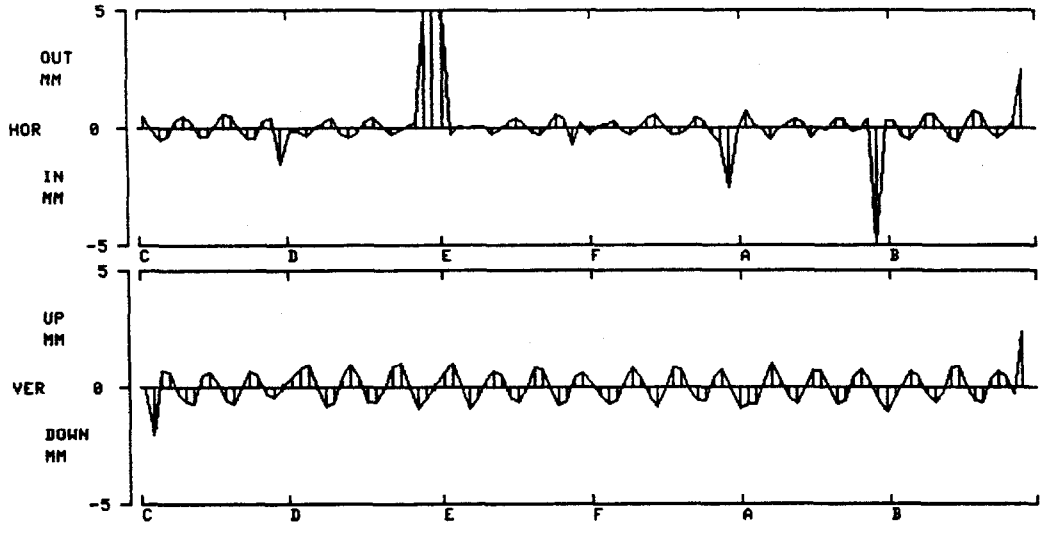

Figure 18. Measured position of the closed orbit at the BPMs after an orbit correction for a collider store in Tevatron at the tune of 19.05. The rms distortion is less than $1mm$. The bump in horizontal plane at E0 is needed for injection and bad BPMs are near A0 and B0.

We conclude that, near integer tunes, the Tevatron closed orbit can be corrected with the 3-bump correction algorithm and that it remains stable for several hours at tunes of 19.05. This verifies that the fields of the superconducting dipoles and the power supplies of the the correction dipoles are stable enough for collider operation near integer tunes.

5.2 Stopband width and compensation

The stopband width determines how close the working point in tune space can be from a resonance line. The amplitude of the transverse oscillation grows and the particles will be lost on the wall of vacuum pipe when the working point is inside the stopband. Near an integer p, the width δ of the integer stopband due to quadrupole errors is

$$\delta = \frac{1}{2\pi} \mid \int_0^C \beta(s)k(s)e^{2ip\phi(s)}ds \mid \qquad (5-4)$$

where $k(s)$ is the local quadrupole error, $\phi = \phi/\nu$ is the normalized phase advance and C is the circumference, as described in chapter II.

Two independently controlled quadrupole circuits are installed in the Tevatron. Since the width is the magnitude of a complex integral, it needs two independent parameters for the correction.

In the experiment when the tunes are close to 19, resonances of the form $2\nu_h = 38$ and $2\nu_v = 38$ must be controlled. The compensation circuit for the horizontal plane is shown in Fig. 19. Two quadrupole magnets of the same strength but with opposite polarity generate the 38th harmonic component without introducing average component which will give rise to a tune shift.

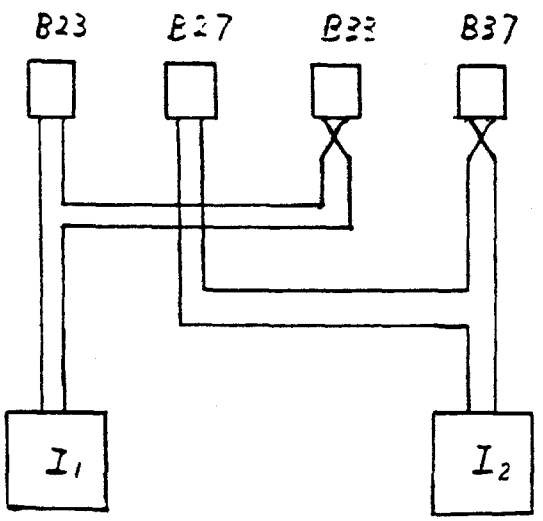

Figure 19. The compensation circuit for the vertical plane. Two quadrupole magnets in series, such as B23 and B33 or B27 and B37, with opposite polarity generate the 38th harmonic component without introducing a tune shift. The phase advance $\delta\psi$ between neighboring quadrupole magnets is 135°. Two current sources, I_1 and I_2, are independently controlled and create two orthogonal vectors in phase space, which give the right phase and magnitude to cancel the integral in Eq (5-4).

5.3 The stopband measurement

Stopband width is measured by moving tune close to the resonance line.

Holding the horizontal tune at 19.09, we moved the vertical tune to 19.025 without any effect on the beam stability. This demonstrates that the half width of the vertical integer stopband at $\nu = 19$ is less than 0.025 with the injection lattice.[16] Similarly, the horizontal integer stopband is measured to be less 0.025.

CHAPTER VI

EXPERIMENT III

PROTON-ANTIPROTON STORES WITH A LARGE TUNE SHIFT

6.1 Working point in tune diagram

As described in chapter III, it is important to choose a working point (ν_h, ν_v) in tune space away from resonances.

During normal Tevatron collider operation, the working point was set to 19.41 and 19.42 in the horizontal and vertical planes respectively. A tune diagram plotted from 19.3 to 19.5 (Fig.20) shows all the resonance lines up to the 7th order in tune space. The working point (19.41, 19.42) is between the 5th and 7th order resonances with a separation of 0.028.

In a P-$\bar{P}$ head-on colliding store, tunes are always shifted up because of beam-beam effects which are equivalent to focusing quads. In the 1989-1990 collider run, a typical store consisted of 6 proton bunches and 6 antiproton bunches (6 on 6) with average bunch intensity of 6.26×10^{10} (protons) and 2.04×10^{10} (antiprotons).[17] The total of 12 crossings arising from 6 on 6 gave a combined antiproton tune shift of 0.02. Since higher luminosity is desirable for colliding experiments, more bunches and higher intensities per bunch are needed. As a consequence, a larger beam-beam tune spread will occur. Since the proton beam is much stronger, the antiproton beam has a larger tune spread. Some antiprotons will cross the 7th order resonance and there will be an intensity loss in the antiproton beam.

Fig.21 is a tune diagram plotted from 19.0 to 19.2 with all the resonance lines up to the 7th order in tune space. The separation from the Nth order resonance to an integer is $1/N$. For example, the separation from the 7th order resonance to 19.0 is $1/7 = 0.143$ which is much larger than the distance between the 5th and 7th.

When the working point is set to (19.05, 19.051), the resonance-free area up to the 7th order is 0.09. The separation of 0.09 is more than four times the maximum tolerable tune spread of 0.02 at the standard tune of 19.42 with six bunches on six bunches.

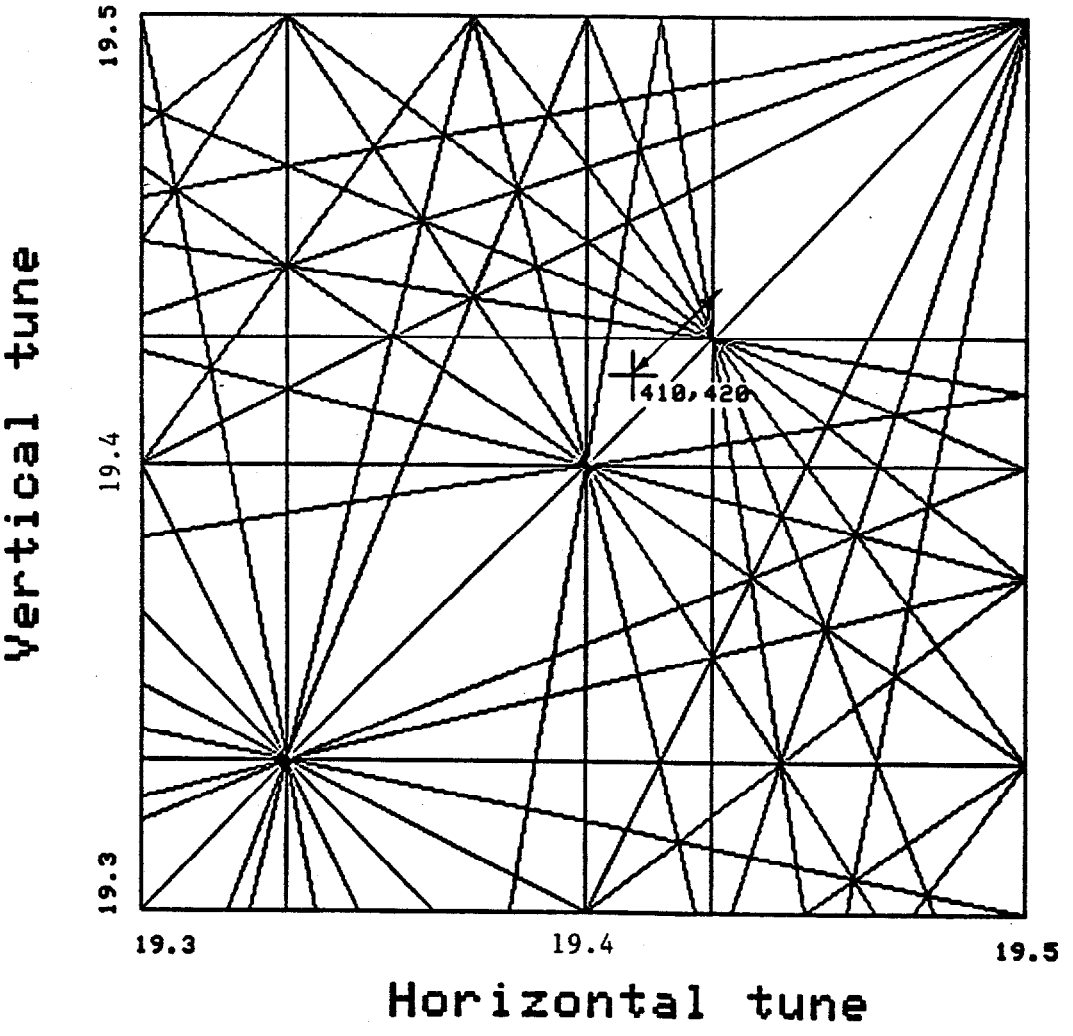

Figure 20. A tune diagram plotted from 19.3 to 19.5 shows all the resonance lines up to the 7th order in tune space. The working point is (19.41, 19.42) and the antiproton tune is shifted upward due to the beam-beam interaction.

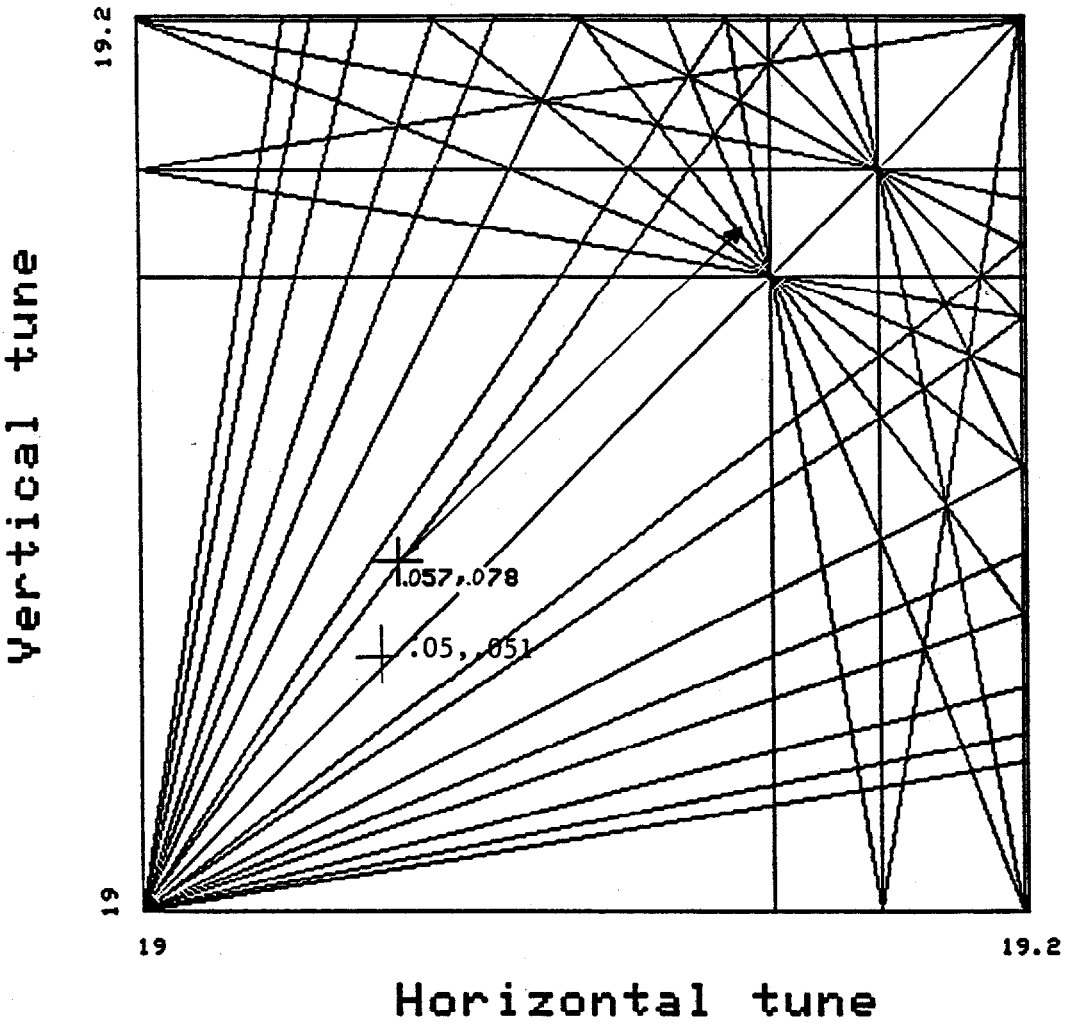

Figure 21. A tune diagram plotted from 19.0 to 19.2 shows all the resonance lines up to the 7th order in tune space. The working point is at (19.05,19.051)

6.2 P-$\bar{P}$ store with large tune shift

One store was attempted which had as its goal a demonstration that the luminosity lifetime would be long even with large tune shifts if the tunes were close to an integer. Unfortunately the proton beam was too strong and the antiproton tune shift was large enough to move the antiproton tunes into a region with many resonances. Nevertheless, the beam lifetimes were quite good, with little emittance growth.

This antiproton-proton store was at 150 GeV with horizontal and vertical proton tunes of 19.06 and 19.08, respectively. There were 36 proton bunches and one antiproton bunch. The total proton intensity was approximately 1.0×10^{12} and the antiproton intensity was 2.5×10^{9}. The proton tunes are thus hardly affected by the antiprotons. On the other hand, the shift in antiproton tune was large. The shifted antiproton tunes are calculated to be 19.14 in the horizontal plane and 19.16 in the vertical plane. This places the antiproton tunes between 6th and 8th order resonance lines. The lifetime of the antiproton bunch was measured to be approximately eight hours when extrapolated from the data in Fig.22. This beam lifetime is unusually long for the calculated tune shift of 0.08.[18]

This long lifetime is understood as a case where the emittance of the low intensity antiproton bunch was small enough to be mostly within the linear region of the strong proton beam-beam force. That is, the antiproton tunes were shifted by .08 but with little tune spread. The proton beam is acting as a quadrupole and the tunes are simply shifted to a region between significant resonances. While the experiment did not address our proposition that regions near integers are more benign, it does seem to be an example of a rather unique operating mode. Namely, there is a good lifetime even with a large tune shift of .08 when the larger proton beam simply acts as a lattice quadrupole at each of the 72 proton-antiproton crossing points.

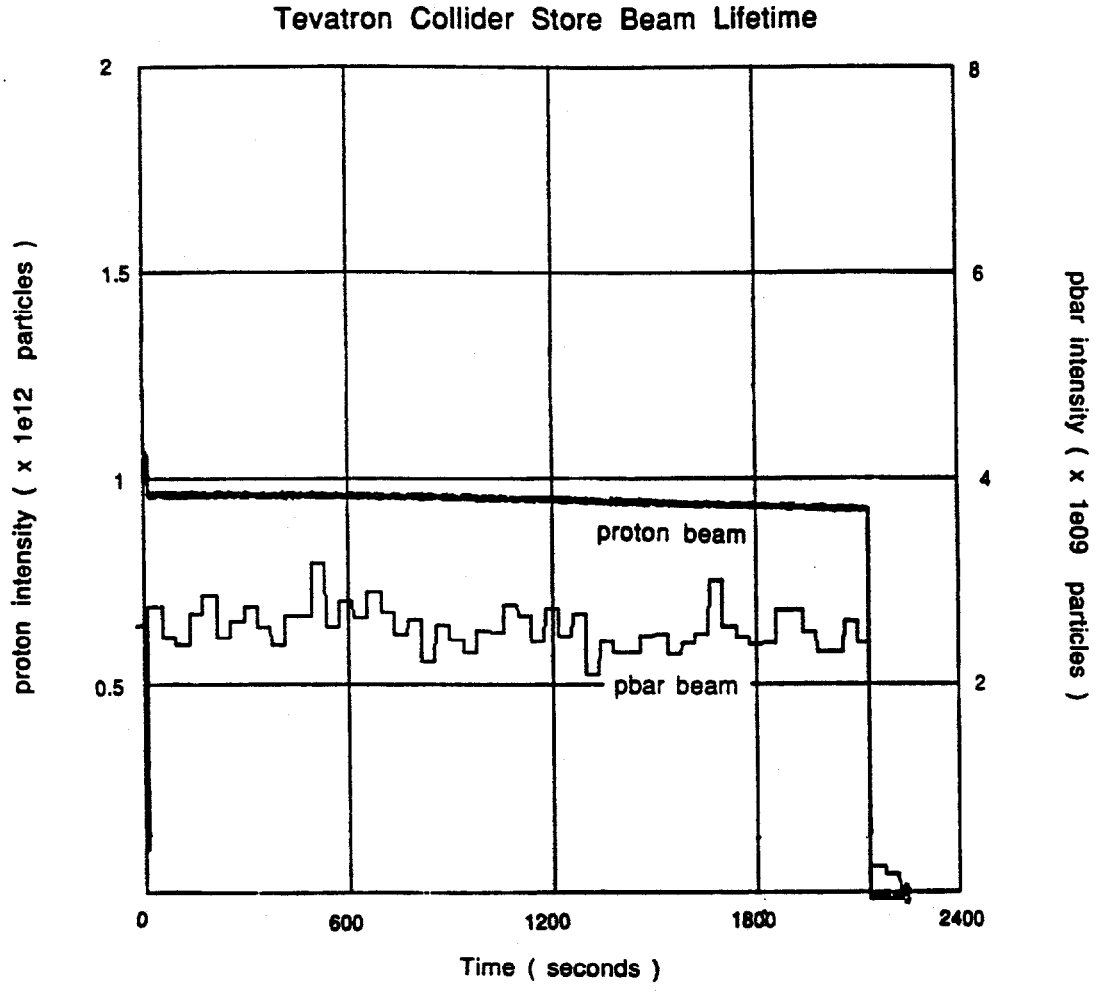

Figure 22. Tevatron Collider antiproton-proton intensities over time for a store with nominal tunes near $\nu = 19.07$.

CHAPTER VII

EXPERIMENT IV

NOISE EFFECTS NEAR INTEGER TUNES

The common mode noise (see 7.2.1) of the main power supply bus is found to be the major cause of emittance growth in the Tevatron near integer tunes where the betatron frequency is low enough to overlap the noise spectrum of the power supply. This condition is true for any machine of large circumference with low betatron frequencies.

7.1 Model of emittance growth

In the presence of tune spread, coherent bunch oscillations become incoherent and this leads to a growth in the beam emittance.[19]

Consider a coherent oscillation of the beam center with amplitude

$$A(t) = \sqrt{2}x(t)\sin(2\pi f_0 \nu t) \qquad (7-1)$$

where $x(t) = x_0 e^{-t/\tau}$, and τ represents the time constant of the rms beam envelope and is directly related to the tune spread. The beam has a normalized emittance ϵ_N (enclosing 95% of particles) and associated beam size σ_b at $t = 0$ given by

$$\sigma_b(0) = [\frac{\beta\epsilon_N(0)}{6\pi(\beta_r\gamma_r)}]^{1/2} \qquad (7-2)$$

where $(\beta_r\gamma_r)$ is the relativistic factor and β is the betatron amplitude function at the point of observation. The amplitude of the betatron oscillation of individual particles is a constant in the case of no interactions with other particles and the field is linear,

$$x^2(t) + {\sigma_b}^2(t) = x^2(0) + {\sigma_b}^2(0) = constant \qquad (7-3)$$

hence

$${\sigma_b}^2(t) = {\sigma_b}^2(0) + {x_0}^2(1 - e^{-2t/\tau}) \qquad (7-4)$$

or

$$\epsilon_N(t) = \epsilon_N(0) + \frac{6\pi(\beta_r\gamma_r)}{\beta}{x_0}^2(1 - e^{-2t/\tau}) \qquad (7-5)$$

so that

$$\frac{d\epsilon_N(t)}{dt} = \frac{6\pi(\beta_r\gamma_r)}{\beta}\frac{2}{\tau}x^2(t) \qquad (7-6)$$

To find out the relation between τ and the tune spread $\Delta\nu$, take the Fourier transform for the complex form of Eq. (7-1).

$$\mathcal{F}\{\sqrt{2}x_0 e^{-t/\tau}e^{-j\omega_0 t}\} = \frac{\sqrt{2}x_0}{(\omega - \omega_0) - j/\tau} \qquad (7-7)$$

here j is $\sqrt{-1}, \omega_0 = 2\pi f_0 \nu_0$ and $\omega = 2\pi f_0 \nu$. We may identify the amplitude FWHM of the resonance

$$\Delta\omega = \frac{\sqrt{12}}{\tau}$$

or the tune spread as

$$\Delta\nu = \frac{\sqrt{12}}{2\pi f_0 \tau} \qquad (7-8)$$

Substituting for τ yields

$$\frac{d\epsilon_N(t)}{dt} = \frac{4\sqrt{3}\pi^2 f_0(\beta_r\gamma_r)\Delta\nu}{\beta} x^2(t). \qquad (7-9)$$

7.2 Emittance growth due to common mode noise

7.2.1 Noise spectrum.

Common mode noise on the main power supply bus is the subject of study in this chapter. The common mode noise refers to the noise on the floating supply bus relative to ground and "common mode" is borrowed from electronics.

Early studies of emittance growth in the Tevatron showed that the common mode noise on the main power supply bus did not lead to problems at tunes near 19.42.[20] The measured noise at the betatron frequency was much smaller than the one at lower harmonics of the 720 Hz which comes from the six phase full wave SCR circuit of the main power supply.

Fig.23 is the spectrum of common mode noise on the power supply which powers the magnet bus current during a store. The spectrum shows a spike at 180 Hz due to the SCR circuit, which is not fully balanced, and its harmonics decay exponentially as the frequency increases.

The betatron frequency is the product of the revolution frequency and the fractional part of the tune. For a tune of 19.42, the betatron frequency is approximately $20kHz(49kHz \times 0.42)$ where the noise is negligible, while for a tune of 19.05, the betatron frequency is approximately 2.3 kHz and the noise is strong enough to cause emittance growth. [21]

7.2.2 Injected noise.

To study the relationship between common mode noise on the bus and beam emittance growth, different levels of common mode noise in the betatron frequency range were injected into the dipole magnet power supply bus. The growth rate of stored beam emittance near the integer tune linearly increases as a function of the square of common mode noise voltage. As described in Eq.(7-6) the growth rate in the beam emittance is proportional to the square of the amplitude of the coherent oscillation of the beam center and the amplitude is proportional to the noise voltage.

Fig.24 shows this linear relationship for a store in the Tevatron for a tune of 19.10.

7.2.3 Suppressed noise.

A suppression circuit for the common mode noise was designed and built to reduce the noise level and to lower the emittance growth rate. A block diagram of the suppression circuit is shown in Fig.25.

When installed on the dipole magnet current power supply in the Tevatron, the suppression circuit reduced the common mode noise by 10 to 15 dbv. Fig.26

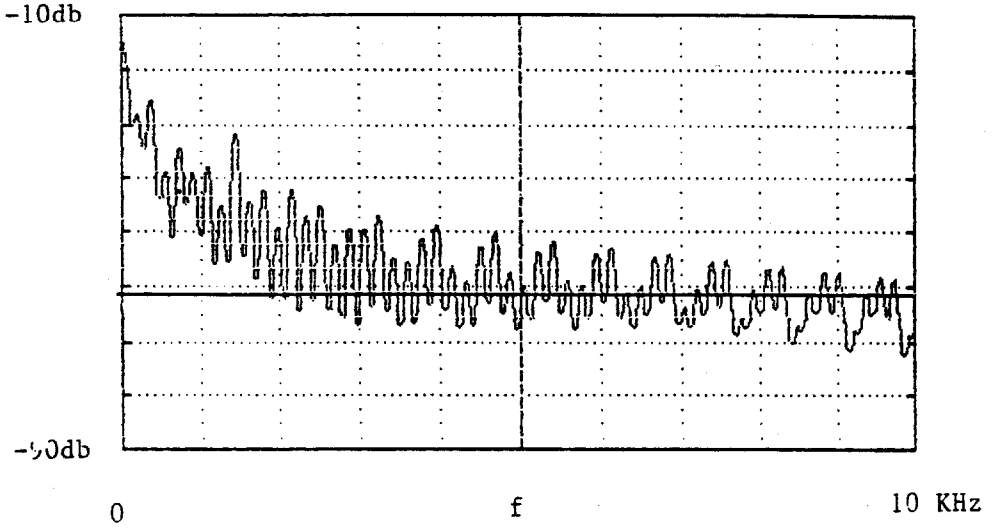

Figure 23. The spectrum of common mode noise on the power supply for the magnet bus current during a store.

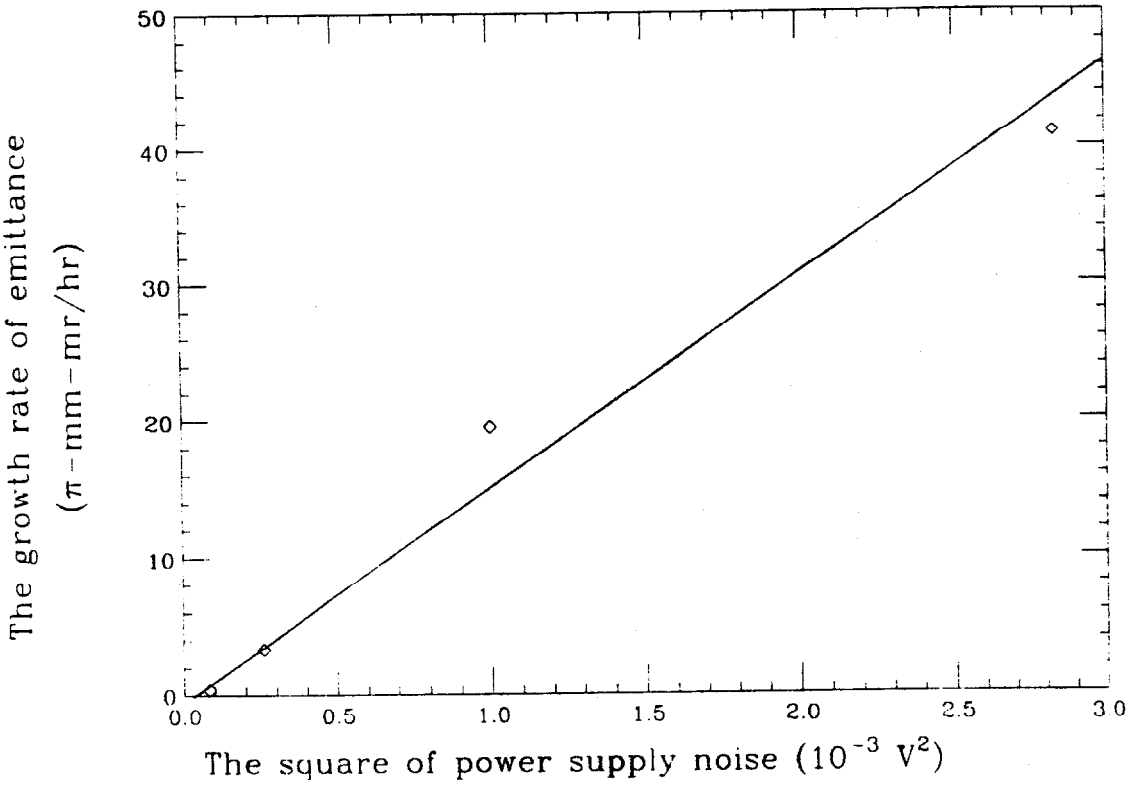

Figure 24. The growth rate of stored beam emittance near the integer tune of 19.10 linearly increases as a function of the square of common mode noise voltage

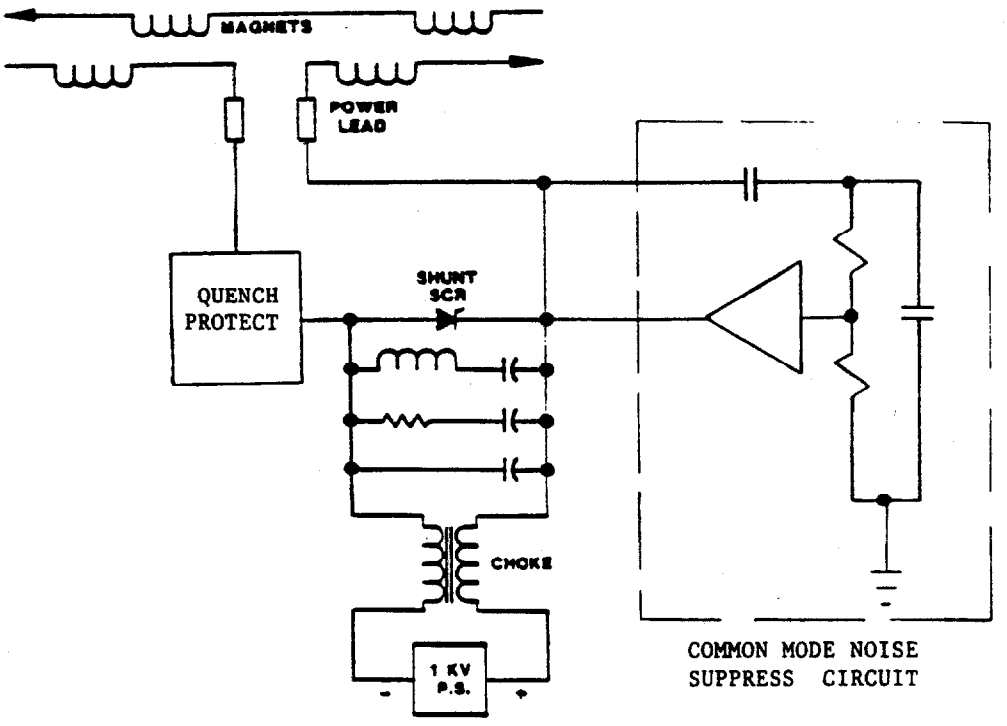

Figure 25. Diagram of the noise suppression feedback circuit. The circuit is outlined by the dashed line. The power leads are connected to the main power supply. A passive filter was also used as shown.

shows noise spectrum in the frequency range from 1 to 4 kHz when the circuit is turned on and off.

The emittance of the stored beam in the Tevatron is measured as shown in Fig.27. The growth rate changed approximately by a factor of two in each plane when the noise suppression circuit was energized. One would have expected a factor of 10 from the 10 db reduction in noise voltage. This suggests strongly that other emittance growth mechanisms become dominant, resulting in a smaller reduction than expected.

7.3 Mechanism of the emittance growth

One possible mechanism of the emittance growth is that the stored beam in the Tevatron is shaken by a fluctuation of the dipole magnetic field. A fluctuation of the dipole components of magnetic field is found inside a test Tevatron dipole magnet when the common mode voltage is applied to the magnet coil bus.

Fig.28 shows the circuit for the measurement in Magnet Test Facility(MTF) at Fermilab. A Tevatron dipole magnet is tested under common mode excitation. A special test pickup coil is placed inside the vacuum pipe of the Tevatron dipole magnet and connected to a phase-lock amplifier which eliminates all frequencies of the noise but the signal frequency. The magnetic field measured inside the magnet is identified as dipole components in the frequency range up to 50 kHz. The field strength is found to be constant along the axis of the vacuum pipe by moving the test pickup coil along the axis. The dipole magnetic field *vs.* the common mode exciting voltage is shown in Fig.29.

The typical common mode ripple of the magnet power supply in the Tevatron is 50 mV in the frequency range from 1 to 4 kHz. Using the model discussed in the beginning of this chapter, one gets an emittance growth rate of 20 $\pi(mm)(mr)/hour$ per magnet for the beam stored with a tune of 19.05.

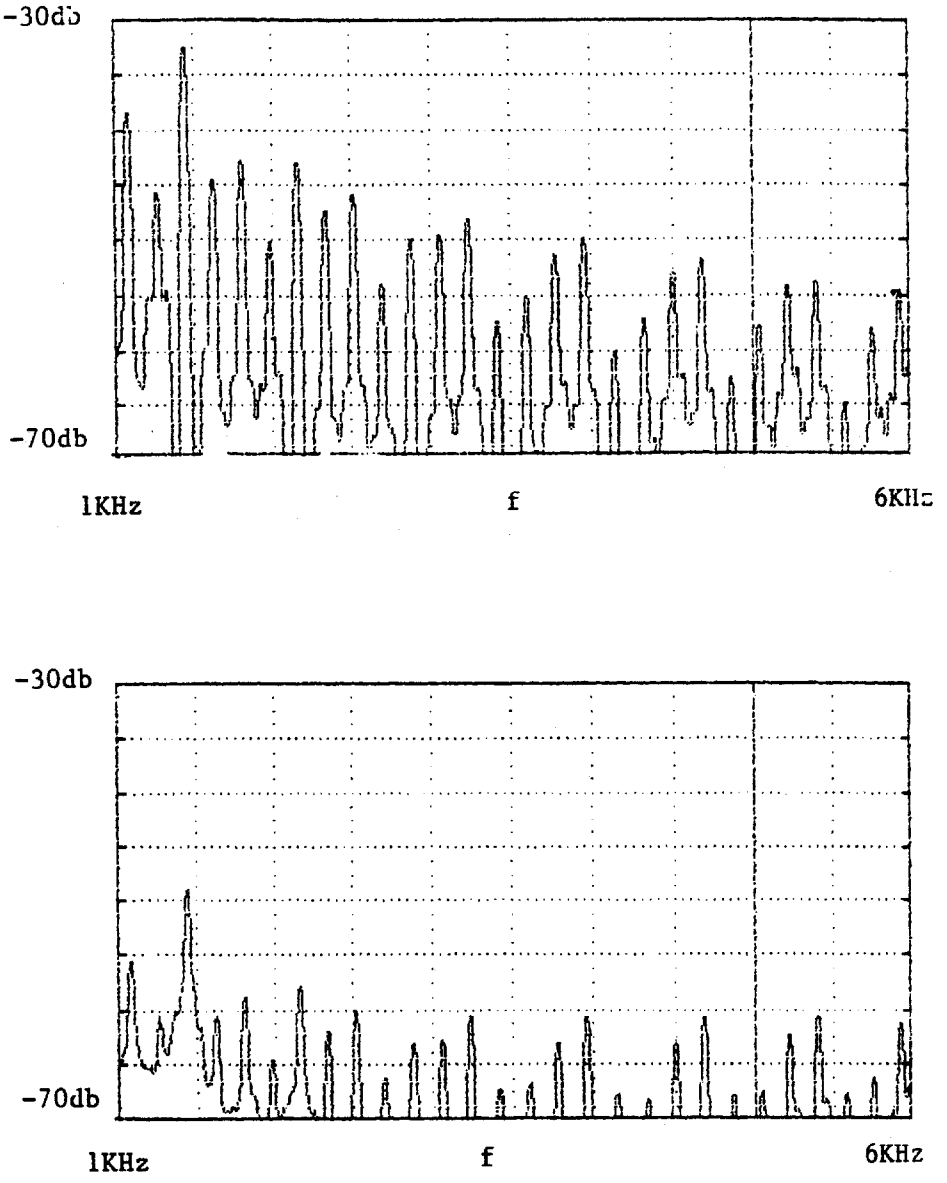

Figure 26. Tevatron main bus power supply noise spectrum with the noise suppression circuit off (top plot) and on (bottom plot). Vertical scale is 5 db/div. The frequency bandwidth is 47.7 Hz. The frequency ranges from 1 kHz to 6 kHz.

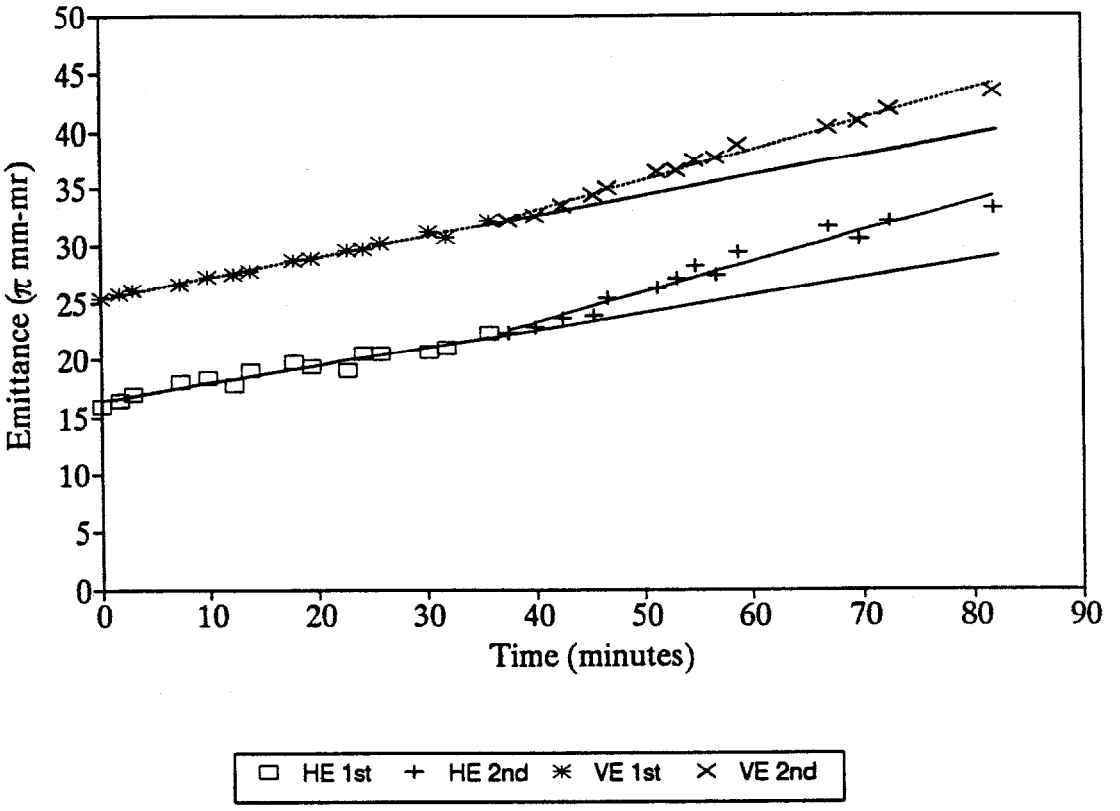

Figure 27. Emittance measurements for a store with the noise suppression circuit connected from 0 to 37 minutes and then disconnected. The upper curve is a measurement of the vertical emittance and the lower is the horizontal emittance. Tunes are 19.05.

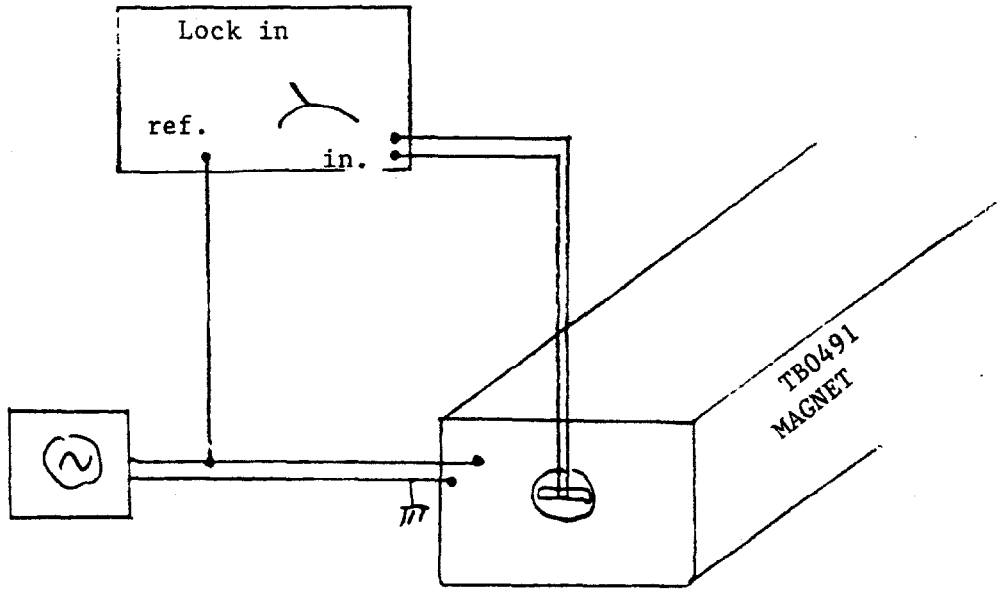

Figure 28. The circuit for the measurement in Magnet Test Facility at Fermilab.

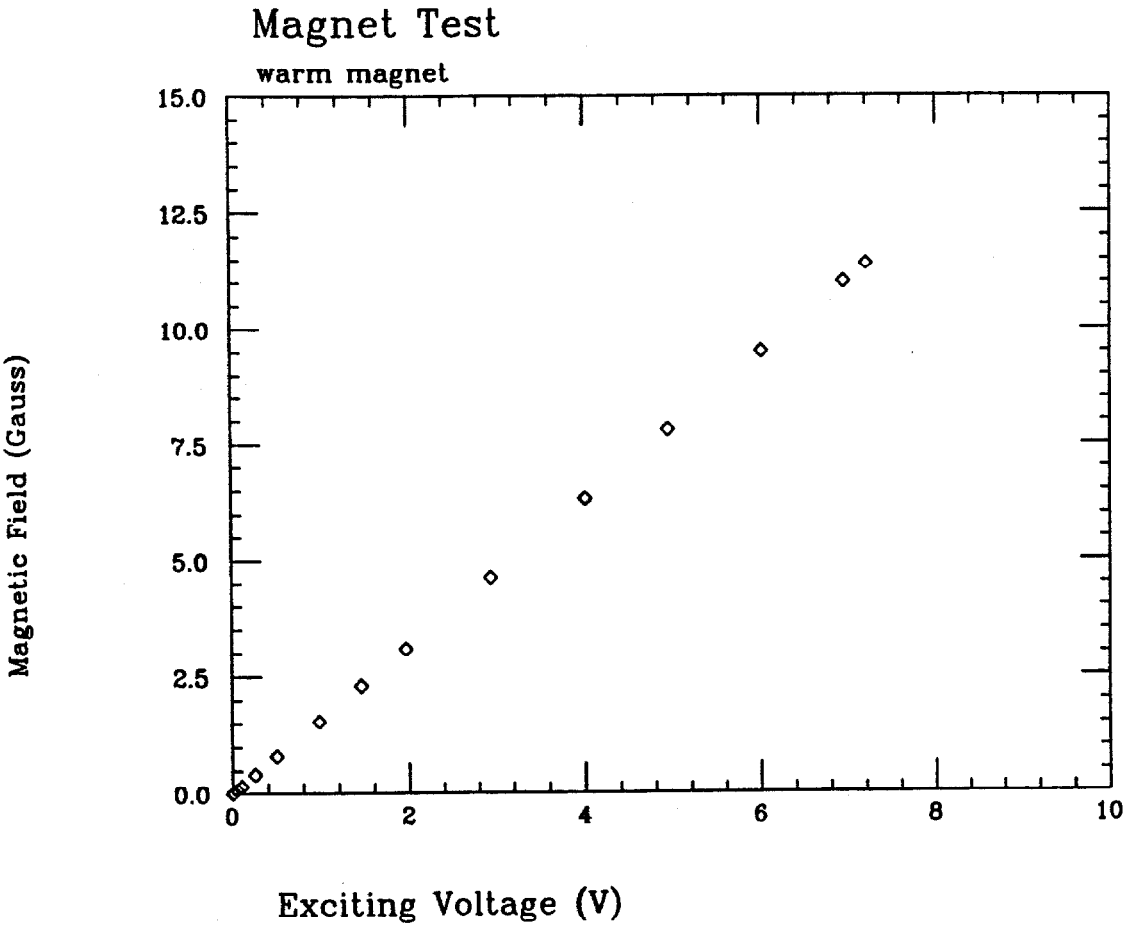

Figure 29. The dipole magnetic field *vs.* the common mode exciting voltage in a Tevatron superconducting magnet.

There are a total of 774 dipole magnets in series in the Tevatron bus. Although the test at MTF shows no common mode decay in a single dipole magnet, the measurement on the Tevatron superconducting magnet bus in the tunnel shows the decay on the bus. The decay is shown in Fig.30 as a function of frequency. The common mode ripple starts at the power supply in the magnet bus and decays as it passes through the chain of magnets, behaving as a damped transmission line.

For the frequency of 2 kHz, the entire bus is equivalent to 17 magnets. Therefore, we should have a growth rate of 0.058 $\pi(mm)(mr)/hour$ for the beam stored in the Tevatron with a tune of 19.05. This result is consistent with the measured value in Fig.27.

With the feed back circuit, the emittance growth rates at tunes near 19.06 are expected to be similar to those seen during early days of Tevatron Collider operation with tunes 19.41. This is based on the improvement due to the relativistic factor and on the character of the SCR supplies, with operation at 900 GeV. Since the emittance is equal to the ϵ_N/γ_r, the emittance at 900 GeV is equal to one sixth of the emittance at 150 GeV. The ripple of power supply at 900 GeV is half of the ripple at 150 GeV, because SCR supply is fully conductive at 900 GeV and is inducing less ripple.

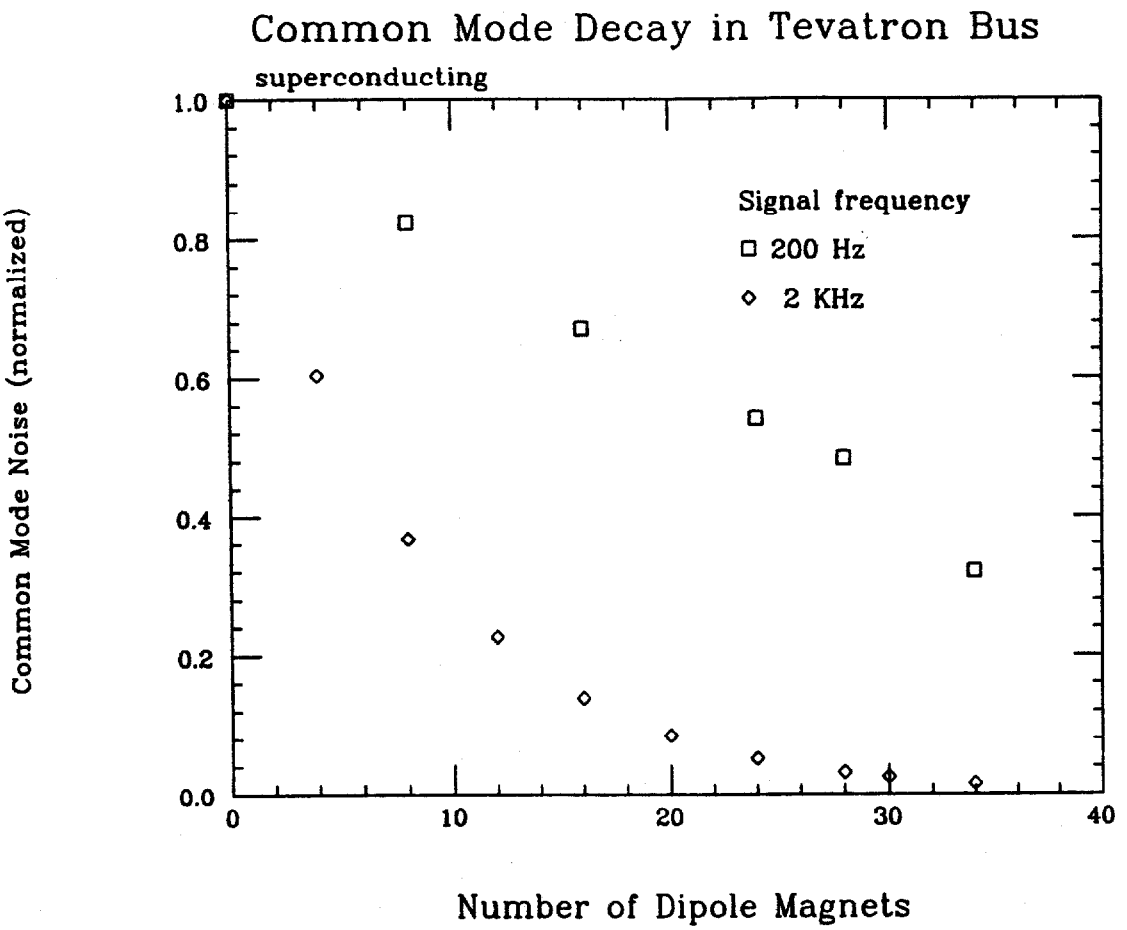

Figure 30. Noise propagation in the chain of magnets in the Tevatron. Measurements for a signal frequency of 200 Hz and 2 KHz are shown.

CHAPTER VIII

SUMMARY AND CONCLUSIONS

Experiments have been performed at the Tevatron collider at Fermi National Laboratory to investigate the feasibility of operating a hadron collider with betatron tunes near integer values. These experiments investigated the benefits and difficulties associated with such a mode of operation and solved some of the associated practical problems.

The results of the experiments indicate that there is no fundamental reason not to have hadron colliders with tunes close to integers. In hadron colliders, the large resonance-free area in tune space available near an integer is an advantage for allowing large beam-beam tune spreads. Keeping the beam tunes in regions free of low order resonances is essential for minimizing the emittance growth and maximizing luminosity lifetime.

Two practical problems associated with betatron tunes near an integer value have been investigated in some detail. The first is the additional strong dependence of the closed orbit on errors in the dipole fields and quad alignment. With a program to correct the orbit distortion and the technological advances in control hardware, this practical problem was found to be easily solvable.

The second practical problem was the increased sensitivity to power supply noise resulting from the lower betatron frequency. Unexpectedly, the dominant source of emittance growth was found to be common-mode noise on the main power supply bus. Measurements on a test dipole magnet showed that the common-mode noise generates a dipole field in the magnet. Measurements of the transmission of the common mode noise along the magnet string furnished a model needed to predict the emittance growth rates, in agreement with those measured rates.

A feed-back circuit was designed and constructed to reduce the common-mode noise on the main bus and was used successfully to reduce the emittance growth rate by a factor of two in each plane. This improvement was less than

expected from the common-mode noise level seen on the bus, indicating that other mechanisms of emittance growth are important.

With the feed back circuit, the emittance growth rates at tunes near 19.06 are expected to be similar to those seen during early days of Tevatron Collider operation with tunes 19.41. This is based on the improvement due to the relativistic factor and on the character of SCR supplies, with operation at 900 GeV.

The new working point near an integer value in tune space allows a tune shift four times greater than the one currently allowed with the normal Tevatron working point and could theoretically increase the maximum luminosity by a factor of sixteen.

BIBLIOGRAPHY

[1] Tevatron I Design Report, Fermilab, September 1984.

[2] "The CDF Detector", Nuclear Instruments and Methods in Physics Research A271 (1988) 378-403.

[3] D.H. Perkins, High Energy Physics, Addison-Wesley Pub. Co.,1982.

[4] J. D. Jackson, Classical Electrodynamics, John Willey & Sons, New York, 1975.

[5] E. Eichten, et al. "Supercollider Physics", Reviews of Modern Physics, Vol.56 No.4, 1984, pp579.

[6] Private conversation with R. Johnson.

[7] SSC Central Design Group, "Conceptual Design of the Superconducting Super Collider", 1986.

[8] R.P. Johnson and P. Zhang,"A New Tevatron Collider Working Point Near the Integer", Proceedings of the 1989 IEEE Particle Accelerator Conference, Vol. II, p.806

[9] D.A. Edwards and M.J. Syphers, "An Introduction to the Physics of Particle Accelerators", AIP Conference Proceedings, No. 184, 1989, pp. 2-189.

[10] E. Courant and H. Snyder, "Theory of the Alternating-Gradient Synchrotron", Annals of Physics, Vol. 3, 1958, pp. 1-48.

[11] L.R. Evans and J. Gareyte,"Beam-Beam Effects", CERN Accelerator School, Sept. 1985, CERN 87-03,Vol. I,p.159.

[12] A.W. Chao, "Coherent Instabilities of a Relativistic Bunched Beam", AIP Conference Proceedings No. 105, 1983, pp. 353-523.

[13] S. Ohnuma, "Accelerator Physics", Lecture Notes, University of Houston, 1987.

[14] Private conversation with R. Johnson.

[15] N. Gelfand, R. P. Johnson, P. Zhang, "Comparison of Tevatron Lattice Measurement with Calculations Based on Measured Magnetic Fields", Proceedings of the 1989 IEEE Particle Accelerator Conference, p. 1427.

[16] P. Zhang, "Integer Tunes Study in the Tevatron", Fermilab EXP-168,1989

[17] N. Gelfand, "Characteristics of the Beam During Collider Run II", unpublished.

[18] P. Zhang, C. Ankenbrandt, D. Finley, G. Goderre, R.P. Johnson, and D. Siergiej, "Prospects for Tunes near the Integer at the Fermilab pbar-p Collider", Proceedings of the 1991 IEEE Particle Accelerator Conference, to be published.

[19] R. Shafer, "Emittance Growth Due to Coherent Betatron Oscillations" 1986. unpublished.

[20] G. Jackson, D. Finley, R.P. Johnson, Q. Kerns, J. McCarthy, R. Siemann, P. Zhang, "Luminosity Lifetime in the Tevatron", 1st European Particle Accelerator Conference 1988, p. 556.

[21] P. Zhang, R.P. Johnson, M. Kuchnir, D. Siergiej and D. Wolff, "Common Mode Noise on the Main Tevatron Bus and Associated Beam Emittance Growth", Proceedings of the 1991 IEEE Particle Accelerator Conference, to be published.